

## Article

# Deep Subsoil Storage of Trace Elements and Pollution Assessment in Mountain Podzols (Tatra Mts., Poland)

Joanna Beata Kowalska <sup>1,\*</sup>, Michał Gąsiorek <sup>2</sup>, Paweł Zadrożny <sup>2</sup>, Paweł Nicia <sup>2</sup>  
and Jarosław Waroszewski <sup>1</sup>

<sup>1</sup> Institute of Soil Science and Environmental Protection, Wrocław University of Environmental and Life Sciences, Grunwaldzka 53, 50-357 Wrocław, Poland; jaroslaw.waroszewski@upwr.edu.pl

<sup>2</sup> Department of Soil Science and Agrophysics, University of Agriculture in Krakow, al. Mickiewicza 21, 31-120 Krakow, Poland; michal.gasiorek@urk.edu.pl (M.G.); pawel.zadrozny@urk.edu.pl (P.Z.); pawel.nicia@urk.edu.pl (P.N.)

\* Correspondence: joanna.kowalska@upwr.edu.pl

**Abstract:** Research highlights: this article refers to the deep storage of trace elements as a result of the podzolization process under different types of vegetation cover. This is also an attempt to trace differentiation in the distribution of trace elements in mountain soils under the podzolization process. Background and objectives: we focused on estimating whether the podzolization process of soils under various vegetation covers led to the deep storage of trace elements in the subsoil. Furthermore, the potential contamination of studied soils with trace elements using pollution indices was assessed. Materials and methods: in thirteen soil profiles under three different vegetation types, chosen chemical–physical properties, e.g., organically bonded and active forms of Al and Fe, podzolization indices, and trace element content (Cd, Pb, Zn, Cu, Cr, and Ni) were analyzed. Additionally, pollution indices, such as Geoaccumulation Index, Potential Ecological Risk, Pollution Load Index, and Contamination Security Index, were calculated. Results: the distribution of Al and Fe varied among the soil profiles, suggesting different rates of podzolization processes that were partially dependent on the type of vegetation. Exceptionally high values of Al<sub>o</sub> and Fe<sub>o</sub> were noted in profiles P1 and P2 (1.53% and 2.52% for Al<sub>o</sub>, and 2.13% and 1.46% for Fe<sub>o</sub>, respectively) in horizons Bs and BsC under *Plagiothecio-Piceetum taricum*. Some of the soils showed the expected distribution of trace elements as the result of the podzolization process revealed their accumulation in the spodic horizon. Moreover, four different patterns of trace element distribution were recognized. Often, the accumulation of trace elements occurred in Bs/BsC horizons, e.g., in case of Zn soils P8, P9, and P10, which reached 65.8, 68.0, and 72.30 mg·kg<sup>-1</sup>, respectively. However, there were no large differences in trace element content in soils independent of the vegetation type. The pollution indices in most samples confirmed lack of contamination with trace elements. Only several soil horizons were moderately polluted and showed deterioration of soil quality or very low severity. Conclusions: in the majority of studied soils, the podzolization process resulted in the deep storage of trace elements, i.e., the accumulation of spodic horizon; however, in certain cases, it might have been related only to the different lithology, and appeared as anomalies not related to the dominant soil-forming process. Anomalies were characterized by a much higher content of trace elements in the BsC horizon compared to the upper O horizons. Obtained data of trace elements, as well as values of pollution indices, did not indicate pollution. This lack of pollution was related to localization of soils within a topographic barrier that protected them from the deposition of potential trace element-rich pollution.



**Citation:** Kowalska, J.B.; Gąsiorek, M.; Zadrożny, P.; Nicia, P.; Waroszewski, J. Deep Subsoil Storage of Trace Elements and Pollution Assessment in Mountain Podzols (Tatra Mts., Poland). *Forests* **2021**, *12*, 291. <https://doi.org/10.3390/f12030291>

Academic Editor: Christopher Weston

Received: 5 February 2021

Accepted: 1 March 2021

Published: 3 March 2021

**Publisher's Note:** MDPI stays neutral with regard to jurisdictional claims in published maps and institutional affiliations.



**Copyright:** © 2021 by the authors. Licensee MDPI, Basel, Switzerland. This article is an open access article distributed under the terms and conditions of the Creative Commons Attribution (CC BY) license (<https://creativecommons.org/licenses/by/4.0/>).

**Keywords:** podzolization; parent material; trace elements; mountain soils; vegetation cover; pollution indices; Tatra Mts

## 1. Introduction

Podzols are the direct effect of a podzolization process, which assumes the release of iron and aluminum oxides, as well as complexes of organic acids from the eluvial horizon (albic material) downward the soil profile, into the illuvial (spodic) horizon [1–4]. The podzolization process reveals different intensity, especially in mountain areas, where many factors may influence its rates [2,5].

Formation of Podzols in the mountain areas is mainly driven by cool and humid climate conditions, topography, as well as specific vegetation [1,3,6–15]. It is widely accepted that coniferous forests promote the formation of proper Podzols [6]. According to Zwanzig et al. [15], *Ericaceae* and some oak species may increase the podzolization rates. Furthermore, Musielok et al. [10] stated that the combination of berry (*Vaccinium* sp.) and mosses (*Polytrichum strictum* and *Sphagnum* sp.) might facilitate the podzolization process even on calcareous materials.

Together with the leaching of organic and inorganic substances, except Fe and Al, other trace elements are involved in the transport within the profiles of Podzols and accumulate in the illuvial horizons [16]. Different rates of the podzolization process under various vegetation covers may be expected, thus intensity of trace elements mobilization in spodic horizons can vary among Podzols [4]. Nonetheless, deep storage of trace elements, originating from natural sources in the subsoil of Podzols, is a fact, and may involve storage of pollutants.

Mountain soils, in general, are very vulnerable to accumulation of contaminations as they form “orographic barrier” that limit and stop air masses, which might lead to increase retention of pollutants, such as trace elements [17–19]. Many studies point out that the southern mountainous part of Poland is extremely exposed to contamination, although it is not situated in the center of pollutant emissions. The main reason of anthropogenic pollutions is long-distance transport, including transboundary sources [19,20]. The example of such area, highly exposed on the trace elements pollution, are Tatra Mts.—the highest mountain range in the Carpathians. Some studies, based on various types of soils in Tatra Mts. and surrounding areas, confirmed the pollution with trace elements, e.g., [18,21,22]. These authors reported that high, unnatural values of trace elements could be caused by various anthropogenic activity from industrial plants, mine, and areas of intensified transport that might be located in the Upper Silesia region (to the west from Polish Carpathian), but also related with many industrial facilities on the Slovak side of Tatra Mts., mostly mining activities [23]. Similar findings and proof of long-distance pollutants transport was noted by the authors dealing with the soils in the surrounding regions of Tatra Mts., but also in other Carpathians ranges, e.g., Little Beskids [24], and in the Sudety Mts., e.g., Karkonosze Mts. [19].

In view of the above, it seems that soils in Tatra Mts. are exposed to the accumulation of trace elements. The assessment of pollution in mountain areas is very important. Up until now, there have been few, detailed analyses based on pollution indices on soils from Polish Carpathians Mts., e.g., [25]. According to many authors, it seems reasonable to track not only the total content of trace elements, but also use favorable pollution indices [26–28] to comprehensively evaluate the degree of contamination, or its lack, in the various ecosystems [28,29]. They may reflect the dynamics of pollution changes that seem important in the context of the functioning of sensitive environments [20,30].

The influence of the podzolization process on the deep storage of trace elements in the soil profile, as well as the influence of external factors, such as human activity, have never been comprehensively combined in one research study so far. Therefore, we decided to (i) estimate if the podzolization process of soils under various vegetation covers leads to the deep storage of trace elements in the subsoil, and (ii) assess the potential contamination of studied soils with trace elements using pollution indices.

## 2. Materials and Methods

### 2.1. Study Area

The Tatra National Park (TPN) was founded in 1954 in the area of the Tatra Mts., which are the highest and only alpine-type mountain massif within in the Polish Carpathians (Figure 1). TPN, together with TANAP (Tatranský Národný Park, Slovakia) are on the list of the World Network of Biosphere Reserves [31]. The geology of the Tatra Mts. is dominated by crystalline, mostly igneous (granites, granodiorites) and metamorphic (gneisses, metamorphic shales) rocks. Among them, the carbonate and crystalline rocks and other less resistant Mesozoic rocks are distinguished. These are covered by Eocene sediments and Palaeogene Podhale flysch, which was denuded during the Neogene period [32].

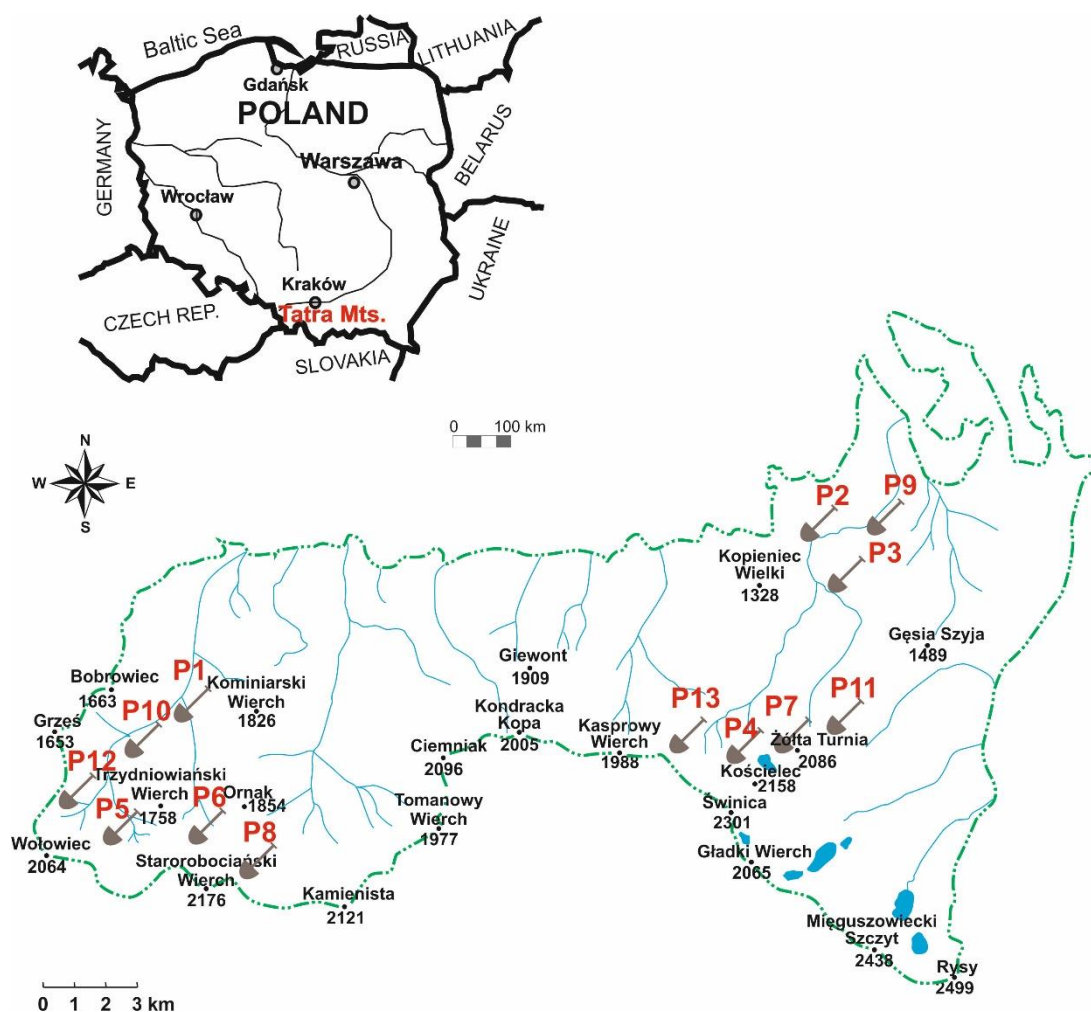


Figure 1. Location of studied soil profiles.

The spatial diversity of the soils in the Tatra Mts. is the result of a close connection with the mountain topography, parent material, and specific hydrological and climatic conditions. According to Komornicki and Skiba [33], 30% of the TPN area is covered by weakly developed soils. Further, nearly 30% is occupied by rendzinas and pararendzinas, about 20% by Podzols, and 10% by brown soil, and about 10% by other types. Podzols occupy large areas in the Eastern and Western Tatra Mts., formed from weathered granitoids, metamorphic slates, acid gneisses, and glacial tills. The podzolization process is favored by cool montane climates with high rainfall, weathered acidic, parent materials, as well as the acidophilic vegetation of alpine and coniferous mountainous forests. Podzols are

strongly acidified, the lowest pH values are found in eluvial horizons (pH 3.0–4.0). The illuvial horizons are slightly less acidic (pH 4.0–5.0) [33].

The Tatra Mts. are generally considered to have a high mountainous, temperate-zone climate. Five climatic zones are distinguished: moderately cool (up to 1150 m a.s.l.), cool (1150–1550 m a.s.l.), very cool (1550–1850 m a.s.l., the upper boundary of the forest), moderately cold (1850–2200 m a.s.l.), cold (above 2200 m a.s.l.—the climatic limit of eternal snow). However, the average temperature of the year varies from +6 °C to −4 °C, which gives an average gradient of 0.5 °C per 100 m. Precipitation in the Tatra Mts. range from 1100 to 1900 mm [34].

The vegetation of the Tatra Mts. is typical for mountain areas, with a zonal layout associated with the changes of climate associated with increasing altitude above sea level [35]. In the lower slopes, up to 1250 m a.s.l., *Dentario glandulosae-Fagetum*, and *Acer pseudoplatanus* L. predominate. Higher, up to a height of about 1550 m a.s.l., *Plagiothecio-Piceetum (tatricum)* and *Polysticho-Piceetum* are the most common. In terms of the undergrowth, *Vaccinium myrtillus*, *Vaccinium vitis-idaea*, *Huperzia selago*, and *Lycopodium annotinum* are commonly present. From 1550 m to about 1800 m a.s.l. (subalpine floor), the mountain pine *Pinus mugo* dominated within which, e.g., *Salix silesiaca*, *Sorbus aucuparia* var. *glabrata* *Vaccinium myrtillus*, and *Vaccinium vitis-idaea* are distinguished [35]. Above, the story of the mountain pine (alpine floor), from 1800 m to about 2300 m a.s.l. *Festuco versicoloris-Seslerietum tatrae* and *Oreochloa distichae-Juncetum trifidi* occur in the undergrowth. Moreover, *Hieracio (alpini)-Nardetum* is quite common. The alpine plant stage in the Tatra Mountains can reach up to 2300 m a.s.l. The vegetation of this stage is dominated by lichens and mosses [35].

## 2.2. Field Study

For this study, thirteen research sites were selected based on the TPN soil map 1:20,000 and arranged under different types, vegetation being a key factor triggering intensity of podzolization and deep storage of the trace elements. The location of studied soil profiles follows the occurrence of Podzols in TPN soil map 1:20,000 [36], frequently present in the eastern and western parts of the mountains, at an altitude from 930 m to 1890 m a.s.l. (Table 1, Figure 1). At each site, soil profile was performed, precisely described, and sampled. In total, 61 soil samples (about 1 kg of soil material per sample) were collected, of which 22 were organic and 39 mineral samples. In all soils, a clear podzolization process was recognized. The northern and northwestern exposures predominated. The slope rating reached from 13° to 50° (Table 1). Soil profiles were divided into three groups (for further data interpretation and statistical analyses) based on type of plant communities: *Plagiothecio-Piceetum tatricum* (soils P1–4), *Vaccinium myrtillus* (soils P5–8), and *Hieracio (vulgati)-Nardetum* (soils P9–13) (Table 1, Figure 1). The chosen location always indicated the representative patch of vegetation cover. The soils were developed from various geological bedrocks, mostly Pleistocene moraine deposits, as well as slope deposits and mantles, representing different geologies: crystalline rocks, such as sandstone and bright quartzite, pegmatite granites, red quartzite sandstones, and white granite gneiss [37]. The field description of the soil profiles was performed using the guidelines for soil description [38]. The color of each horizon was determined using the Standard Soil Color Charts [39]. The soils were classified, according to the World Reference Base for Soil Resources [40], as Podzols with additional principal and supplementary qualifiers (Table 1).

**Table 1.** Location sites, general information and classification of soil profiles.

Profile Number	Altitude a.s.l. (Slope Rating/Exposure)	Landform and Topography *	Parent Material	Vegetation	WRB Classification (WRS, IUSS Working Group 2015)
1	1080 (15°/NNW)	MS	Pleistocene moraine deposits	<i>Plagiothecio-Piceetum (tatricum)</i>	Endoskeletal Albic Podzol (Loamic)
2	1130 (13°/NNW)	MS	Pleistocene moraine deposits		Endoskeletal Albic Podzol (Arenic)
3	1200 (15°/NNW)	MS	sandstone and bright quartzite slope deposits		Episkeletic Albic Podzol (Arenic)
4	1890 (45°/NW)	MS	Pegmatite granite slope deposits		Episkeletic Albic Podzol (Arenic)
5	1360 (15°/N)	MS	Pleistocene moraine deposits	<i>Vaccinium myrtillus</i>	Episkeletic Albic Stagnic Podzol (Arenic)
6	1380 (15°/N)	MS	Pleistocene moraine deposits		Episkeletic Albic Podzol (Arenic)
7	1720 (/50°/NW)	US	red quartzite sandstone slope deposits		Endoskeletal Albic Podzol (Loamic)
8	1770 (45°/NW)	US	white granite gneiss slope deposits		Episkeletic Umbric Podzol (Arenic)
9	930 (15°/N)	MS	Pleistocene moraine deposits	<i>Hieracio (vulgati)—Nardetum</i>	Episkeletic Albic Podzol (Siltic)
10	1210 (15°/SE)	MS	Pleistocene moraine deposits		Endoskeletal Albic Podzol (Loamic)
11	1385 (15°/N)	MS	Pleistocene moraine deposits		Endoskeletal Albic Podzol (Loamic)
12	1590 (45°/NE)	MS	white granite gneiss slope deposits		Episkeletic Albic Podzol (Arenic)
13	1890 (45°/N)	US	Pleistocene moraine deposits		Endoskeletal Albic Podzol (Loamic)

Explanation: MS—middle slope, US—upper slope, \* according to Mokma and Buurman [2].

### 2.3. Selected Physical and Chemical Properties

The soil samples were air-dried and sieved through a certified sieve (2 mm diameter). Particle size distribution was determined using the hydrometer-sieve method [41]. The measurements of potentiometric pH values were performed using a standard combination electrode and a CPI-551 Elmetron pH meter in H<sub>2</sub>O as well as in 1 M KCl solution at a ratio of 1 (soil):2.5 (solution) [41]. Total organic carbon (TOC) content was determined by using potassium dichromate and Mohr's salt [42]. Total nitrogen (TN) content was obtained using the Kjeldahl method [43] on a FOSS Kjeltac™ 8100 apparatus. The base saturation (BS) was calculated from the total exchangeable acidity (EA), and the sum of exchangeable bases such as Ca<sup>2+</sup>, Mg<sup>2+</sup>, Na<sup>+</sup>, and K<sup>+</sup> (TEB), calculated according to van Reeuwijk [41] and analyzed with an ICP-OES Optima 7300 DV optical emission spectrometer. The "organically bound" Al and Fe were extracted with pyrophosphate solution (Al<sub>p</sub>, Fe<sub>p</sub>, C<sub>p</sub>), whereas the "active", Al and Fe were extracted with acid oxalate solution (Al<sub>o</sub>, Fe<sub>o</sub>), according to van Reeuwijk [41]. The organically bound and active forms of Al and Fe were indicated only for the mineral horizons. All of the analyses were performed at University of Agriculture in Krakow (Poland). The content of Al<sub>p</sub>, Fe<sub>p</sub>, C<sub>p</sub>, Al<sub>o</sub>, and Fe<sub>o</sub>, were used for calculation of the selected diagnostic indicators for the spodic horizon as follows: (i) index of Al<sub>p</sub>, Fe<sub>p</sub>, C<sub>p</sub> complex content in the spodic horizon: Al<sub>p</sub> + Fe<sub>p</sub> + C<sub>p</sub> [2]; (ii) molar ratio of organic carbon to the sum of Al<sub>p</sub> and Fe<sub>p</sub>: C<sub>p</sub>/Al<sub>p</sub> + Fe<sub>p</sub> [2]; and (iii) the displacement ratio of amorphous forms of Al<sub>o</sub> and Fe<sub>o</sub>: Al<sub>o</sub> + 0.5 Fe<sub>o</sub> [40].

### 2.4. Content of Trace Elements and Pollution Indices

Content of Cd, Pb, Zn, Cu, Cr, and Ni was determined after wet digestion of soil samples in a mixture of concentrated nitric and perchloric acids (2:1 v/v) [44]. In the solution thus obtained, the content trace elements were detected with the Perkin Elmer Optima 7300 DV spectrometer. Calibration was done using a certified multi-element ICPIV

Merck standard solution. The detection limit was as follows: Cd–0.03; Cr–0.04; Cu–0.2; Ni–0.1; Pb–0.5; and Zn–0.2 ( $\text{mg}\cdot\text{kg}^{-1}$ ).

Based on the trace element contents, four pollution indices were calculated: Geoaccumulation Index ( $I_{\text{geo}}$ ), Potential Ecological Risk (RI), Pollution Load Index (PLI), and Contamination Security Index (CSI) [28]. For the calculation of RI and PLI, the Single Pollution Index (PI) was first necessary [28]. The pollution indices mentioned above allow recognition of the degree of trace element contamination and potential ecological risk, evaluation of the degree of soil degradation due to possible trace elements enrichment, as well as determination of the limit of toxicity, above which adverse impacts on the soil environment is observed [27,28,45,46]. Sometimes, the pollution indices may give more information than the raw data of trace elements and help to assess both the degree of contamination and potential ecological risks [28]. For the calculation of pollution indices, the total content of trace elements from each organic and mineral horizon, as well as geochemical background, were used. The  $I_{\text{geo}}$  allowed for pollution assessment with each, studied trace element [28]; whereas PLI, CSI, RI favored the identification of pollution based on total contamination, with all trace elements under study [28]. The geochemical background for  $I_{\text{geo}}$ , RI and PLI was calculated based on trace element content in the lowermost horizons of studied soils. The lowest horizons were used to assess the possible trace elements contamination—mainly the parent material horizons. BC/C horizons usually revealed natural trace elements content, with lack or non-signs of contamination. For this purpose, the mean content of a given trace element in the lowermost horizon  $\pm 2$  standard deviations was used [47].

### 2.5. Statistical Analysis

Principal component analysis (PCA) was used to reduce the dimensionality of the dataset and summarize the soil properties in large data during the evaluation. The main components were examined based on projection methods. Bartlett's sphericity test was used for the inferential statistics to assess the equality of variance. Kaiser–Meyer–Olkin (KMO) was applied to measure sampling adequacy. PQ stat (version 1.8.0) was used for data analysis and to visualize results in a biplot (a score plot and a loading plot in a single graph). Moreover, the differences between the contents of trace element in the eluvial (E) and illuvial (B) horizons were assessed, based on a non-parametric Mann–Whitney U test using Statistica® software. Statistical analysis was performed at the University of Agriculture in Krakow (Poland).

## 3. Results

### 3.1. Morphological Characteristics of Studied Soils

All soils were characterized by the presence of albic and spodic horizons. The colors of the soil material showed the typical patterns for Podzols and fulfilled the criteria for spodic in illuvial horizons [40]. Generally, the eluvial horizons (AE or E) indicated hues from 7.5 YR to 10 YR values from 3 to 7 and chroma from 1 to 4. Whereas the illuvial horizons showed usually 7.5 YR, 10 YR and rarely 5 YR hue values from 2 to 5 and chroma from 3 to 8 (Appendix A, Table A1). Regardless of the type of parent material, the studied soils were characterized by a high content of rock fragments that generally increased downward the soil profiles, even reaching >80%, where they were dominant (Table A1). Among all studied soils, an abrupt and clear type of boundary predominated especially at the contact of the A/E and E/Bs horizons. Independent of the vegetation cover, the soils were quite similar in terms of soil structure. Most of the studied horizons represented a subangular or angular type of structure. Some of A horizons showed a crumbly type of structure that was well visible in P5, P6, and P11 (Table A1). As is typical, the number of roots decreased with depth in all soils. The consistence changed down the soil profile, from friable in upper soil horizons to very firm in the lowest horizons sampled (Table A1).

### 3.2. Particle Size Distribution

The texture of studied soils did not differ between mineral soil horizons (Figure 2). In general, Podzols have sandy loam, loamy sand, as well as sand textures (Figure 2).

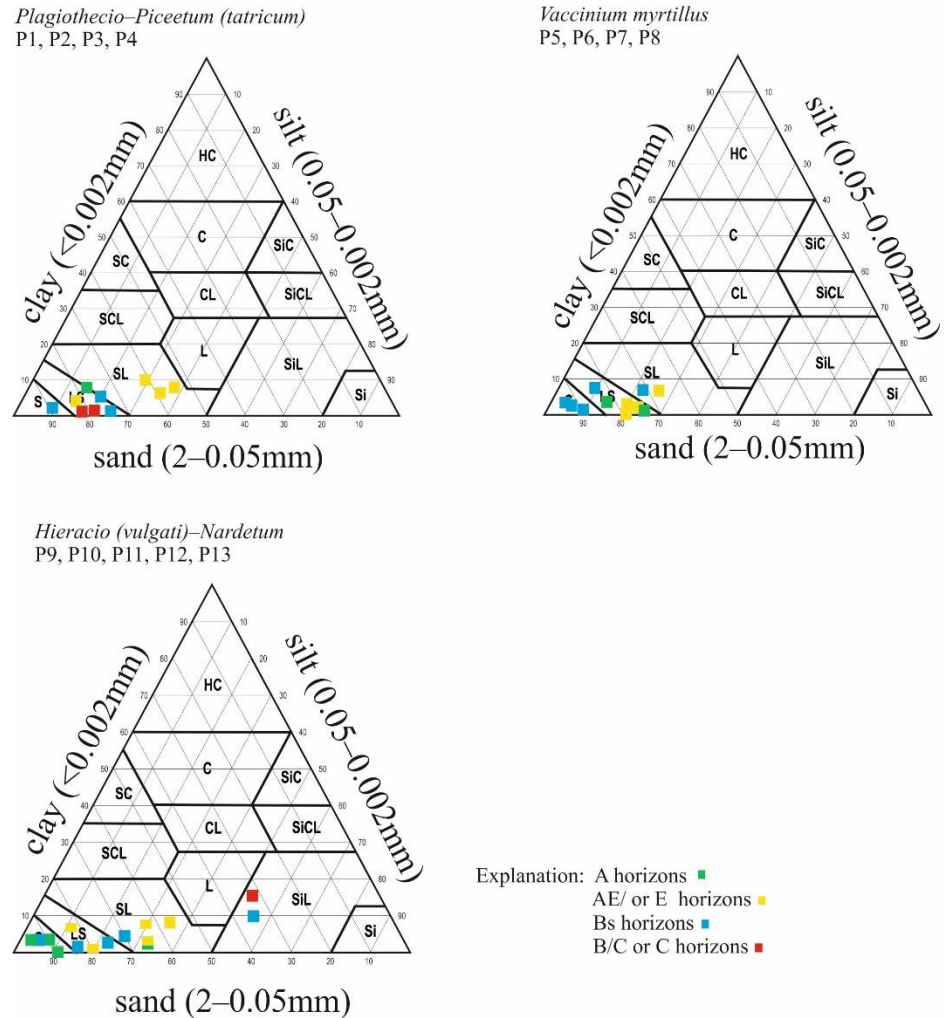


**Figure 2.** Particle sized distribution of studied soils under different vegetation.

Coarse and medium sand content varied between E and Bs/BsC horizons even up to 22–23% (P1 and P4). Only subsoil of profile P9 was finer, where the silt and clay fractions reached 50–54% and 10–18%, respectively (Appendix B, Table A2).

### 3.3. Selected Chemical Properties

Irrespective of the vegetation cover, the reaction of the studied soils ranged from strongly acidic to acidic. The pH values slightly increased towards the down of the soil profile, both in H<sub>2</sub>O and KCl solution. The higher values of pH were noted in soil P10 in the E and BsC horizons (5.7 and 5.8, respectively), which may result from less acidic character of parent material (Table 2). Based on the values of individual ions (Ca<sup>2+</sup>, Mg<sup>2+</sup>, Na<sup>+</sup>, K<sup>+</sup>) as well as TEB, it can be noted that their values undoubtedly decreased down the soil profile, with their highest values in the Ol/Olf and Oh horizons. The values of TEB and the individual cations were comparable in all soil profiles (Table 2). Yet, clearly distinguishable high values of TEB in Ol/Olf horizons were marked in soils P3, P6, P8, and P13 due to a relatively high content of K<sup>+</sup> compared to the other profiles (Table 2). The EA showed quite high values typical for Podzols and acidic soils, generally. The highest values were characterized for the O horizons, which were additionally acidified by the

availability of organic remains with varying degrees of decomposition. The values of EA decreased down the soil profile. Usually, the values of EA in BsC or BC horizons were almost two times lower than the values noted in O horizons (Table 2). In some of the soils, the eluvial horizons showed values close to those determined in the O horizons, e.g., P4, or even exceeded those values, e.g., P5 (Table 2).

**Table 2.** Selected chemical properties.

Profile Number	Soil Horizon	Depth (cm)	Exchangeable Cations											C/N	
			pH		Ca <sup>2+</sup>	Mg <sup>2+</sup>	Na <sup>+</sup>	K <sup>+</sup>	TEB	EA	CEC	BS	TOC		NT
			H <sub>2</sub> O	KCl											
1	Ol	0–10	3.5	2.4	12.4	13.3	1.52	17.54	44.8	203	248	18	379	17.2	22.1
	Oh	10–14	3.7	2.8	1.67	4.42	0.93	4.03	11.0	331	342	3	125	10.5	11.9
	AE	14–27	4.3	3.5	0.28	0.52	0.41	0.82	2.03	265	267	1	27.9	2.20	12.7
	Bs	27–44	4.7	4.1	0.10	0.25	0.26	0.70	1.31	123	124	1	36.0	1.90	18.9
	BC	44–56	4.8	4.3	0.11	0.23	0.21	0.80	1.35	74.3	75.6	2	26.6	1.40	19.0
2	Ol	0–4	3.4	2.3	16.1	9.20	1.07	9.62	36.0	271	307	12	379	18.0	21.1
	Oh	4–8	3.5	2.4	6.65	1.24	0.91	6.60	15.4	314	329	5	181	11.9	15.3
	A	8–18	4.0	3.1	0.48	1.33	0.27	1.13	3.21	231	234	1	45.9	2.60	17.7
	E	18–40	4.9	3.7	0.98	4.82	0.26	0.45	6.51	220	227	3	19.8	0.70	28.3
	BsC	40–70	4.6	4.1	0.04	0.29	0.24	0.64	1.22	78.5	79.8	2	43.8	2.10	20.9
3	Ol	0–4	3.6	2.5	19.4	16.1	1.82	30.4	67.9	203	271	25	373	16.7	22.4
	Oh	4–8	3.4	2.4	3.02	7.25	2.03	6.41	18.7	280	299	6	199	11.9	16.8
	AE	8–12	3.6	2.8	1.07	2.40	0.54	1.79	5.80	212	218	3	61.4	4.10	15.0
	BsC	12–28	4.4	3.8	0.11	0.52	0.26	0.78	1.67	140	141	1	34.1	2.0	17.1
4	Ol	0–2	3.5	2.5	8.45	15.1	0.76	13.5	37.9	263	301	13	328	16.0	20.5
	Oh	2–6	3.5	2.5	8.32	9.66	1.01	8.66	27.6	118	146	19	210	12.2	17.2
	A	6–14	3.8	2.7	2.56	4.49	0.44	3.68	11.1	180	191	6	80.3	5.90	13.6
	E	14–20	4.0	3.0	1.27	1.77	0.42	1.86	5.32	256	262	2	66.7	3.70	18.0
	BsC	20–39	4.5	3.8	0.37	0.60	0.27	1.20	2.44	176	178	1	33.8	2.10	16.1
5	Ol <sub>f</sub>	0–3	3.3	2.8	7.90	10.41	1.05	22.3	41.6	144	186	22	356	7.70	46.3
	A	3–7	3.6	2.6	1.51	2.03	0.37	2.43	6.35	114	121	5	63.4	6.20	10.2
	AE	7–19	3.9	2.9	2.78	1.31	0.28	1.44	5.81	116	122	5	24.7	2.40	10.3
	E	19–37	4.0	2.7	1.40	1.15	0.21	0.92	3.67	159	162	2	9.8	1.00	9.80
	BsC	37–50	4.3	3.5	0.98	0.77	0.21	1.10	3.07	172	175	2	23.5	2.00	11.8
6	Ol <sub>f</sub>	0–6	4.1	2.8	7.35	26.5	0.98	45.9	80.7	152	233	35	378	17.9	21.1
	A	6–11	4.0	3.0	1.25	5.36	0.59	5.69	12.8	152	165	8	84.1	8.10	10.4
	E	11–16	4.2	3.2	1.16	1.56	0.26	2.35	5.33	138	143	4	33.3	3.70	9.00
	BsC	16–39	4.8	4.1	0.28	0.40	0.26	1.25	2.19	67.9	70.1	3	21.3	1.70	12.5
7	Ol	0–3	3.6	2.7	13.1	7.57	0.60	7.46	28.8	229	258	11	341	18.7	18.2
	Oh	3–8	3.7	2.9	6.66	7.50	1.03	7.01	22.2	229	251	9	177	12.1	14.7
	A	8–23	4.4	3.6	1.53	0.80	0.33	1.32	3.98	133	137	3	25.5	2.20	11.6
	E	23–38	4.5	3.5	1.21	1.08	0.48	1.70	4.47	150	155	3	29.8	2.90	10.3
	BsC	38–58	4.6	3.8	0.57	0.68	0.39	1.27	2.91	114	117	2	31.3	2.60	12.0
8	Ol <sub>f</sub>	0–10	3.5	2.6	19.4	22.4	1.19	20.0	63.2	203	267	24	339	13.1	25.9
	AE	10–33	3.7	2.8	2.62	3.47	0.55	3.26	9.89	186	196	5	73.3	4.40	16.7
	BsC1	33–40	4.0	3.1	0.74	1.48	0.41	1.79	4.42	231	235	2	45.4	2.70	16.8
	BsC2	40–60	4.7	4.0	0.75	0.68	0.35	1.12	2.90	110	113	3	30.1	2.20	13.7
9	Ol <sub>f</sub>	0–6	3.8	3.0	2.73	8.23	1.27	9.17	21.4	237	259	8	172	12.6	13.7
	A	6–10	4.6	3.6	1.88	2.40	0.35	2.33	6.96	108	115	6	37.2	4.20	8.90
	E	10–18	4.6	3.7	1.98	0.67	0.23	1.08	3.95	104	108	4	21.9	2.70	8.10
	Bs	18–24	4.7	3.9	1.42	0.63	0.30	0.97	3.32	84.9	88.2	4	31.9	3.70	8.60
	BC	24–60	4.8	3.9	3.20	0.85	0.27	1.18	5.49	93.4	98.9	6	9.50	1.20	7.90
10	Ol <sub>f</sub>	0–2	3.9	3.0	12.2	14.7	0.89	13.3	41.2	135	177	23	213	9.80	21.8
	A	2–6	4.0	3.1	3.21	4.25	0.34	2.93	10.7	118	129	8	49.4	4.50	11.0
	AE	6–23	4.0	3.5	2.13	0.70	0.26	0.86	3.95	40.3	44.3	9	9.80	1.10	8.90
	E	23–45	5.7	4.4	8.67	0.14	0.22	0.35	9.38	10.6	19.9	47	1.30	0.30	4.30
	BsC	45–70	5.8	4.4	2.79	1.58	0.25	0.82	5.44	25.4	30.9	18	14.1	1.30	10.8

Table 2. Cont.

Profile Number	Soil Horizon	Depth (cm)	Exchangeable Cations											C/N	
			pH		Ca <sup>2+</sup>	Mg <sup>2+</sup>	Na <sup>+</sup>	K <sup>+</sup>	TEB	EA	CEC	BS	TOC		NT
			H <sub>2</sub> O	KCl	cmol(+) · kg <sup>-1</sup>					%	g · kg <sup>-1</sup>				
11	Olf	0–3	4.0	3.0	7.90	17.1	1.17	21.0	47.2	161	208	23	355	18.8	18.9
	A	3–8	3.5	3.2	0.92	3.70	0.72	3.91	9.24	148	157	6	59.5	6.10	9.80
	AE	8–16	4.4	3.7	1.28	1.17	0.42	1.68	4.56	121	125	4	29.2	3.80	7.70
	BsC1	16–40	4.7	4.0	1.17	0.39	0.29	0.99	2.84	121	123	2	14.4	2.00	7.20
	BsC2	40–65	4.9	4.2	0.89	0.34	0.26	0.88	2.37	42.4	44.8	5	16.4	1.50	10.9
12	Olf	0–3	3.8	3.0	9.63	5.14	0.43	4.96	20.1	144	164	12	61.5	4.5	13.7
	A	3–26	4.2	3.2	2.38	1.17	0.22	1.73	5.50	146	152	4	22.4	2.4	9.30
	AE	26–43	4.4	3.3	1.68	0.80	0.18	1.46	4.12	172	176	2	14.6	1.5	9.70
	BsC	43–62	4.4	3.6	1.31	0.49	0.24	1.24	3.28	157	160	2	25.2	1.6	15.8
13	OI	0–3	4.3	3.4	16.5	15.4	1.18	28.5	61.5	170	232	27	356.9	21.7	16.4
	Oh1	3–6	4.0	3.3	4.17	7.44	0.77	11.4	23.8	229	253	9	198.4	17.6	11.3
	Oh2	6–20	4.7	4.0	0.25	1.91	0.43	3.39	5.98	195	201	3	114.2	10.3	11.1
	AE	20–50	4.6	3.7	0.43	1.51	0.52	2.39	4.85	125	130	3.73	81.6	8.0	10.2
	BsC	50–70	4.9	4.2	0.08	0.48	0.27	1.17	2.01	61.5	63.6	3.15	60.9	5.2	11.7

Explanation: TEB—total exchangeable bases (=exchangeable Ca + Mg + Na + K); EA—exchangeable acidity; CEC—cation exchange capacity; BS—base saturation percentage; TOC—total organic carbon; NT—total nitrogen.

Regardless of the vegetation cover, the values of cation exchange capacity (CEC) were varied, and included the ranges from 146.6 to 342.3 cmol·kg<sup>-1</sup> and from 20.0 to 267.5 cmol·kg<sup>-1</sup>, in the organic and mineral horizons, respectively. In the case of CEC, the values were quite similar under different plant habitats. There was a downward trend, however, with much lower (more than two times) values of CEC in BsC and BC horizons. The soils were generally characterized by low BS. Organic horizons showed BS values from 3% to 35%, whereas in mineral horizons, values from 1% to 6% dominated. The exception was in soil P10, where especially horizon E indicated relative very high values for BS – 47% (Table 2). The highest values of TOC and TN were in the OI/Olf and Oh horizons (61.5 to 379.9 g·kg<sup>-1</sup>) and rapidly decreased with the depth. The values of TOC and TN were comparable in all of studied soils, nonetheless in soil P13, showed quite high values, even in mineral horizons (up to 60.9–81.6 g·kg<sup>-1</sup>). Neither TOC nor NT showed a depletion of content of these elements in the eluvial horizon and enrichment in the illuvial horizons (Table 2).

### 3.4. Podzolization Indices

Regardless of the type of the vegetation cover, the contents of Al<sub>p</sub>, Fe<sub>p</sub>, C<sub>p</sub>, Al<sub>o</sub>, and Fe<sub>o</sub> were very diverse within the soil profile; this suggested that the rate of the translocation of those elements along the solum was varied too. Nonetheless, some obvious trends for Podzols were noted. In case of each element (Al<sub>p</sub>, Fe<sub>p</sub>, C<sub>p</sub>, Al<sub>o</sub>, Fe<sub>o</sub>), a slight decrease was observed in the eluvial horizons, while in the BsC horizons clear enrichment was noted compared to the uppermost horizons (AE or E, Table 3). The content of C<sub>p</sub> in soil P3 was higher in AE horizon than in BsC horizon. Both organically bound and active forms of Al and Fe showed approximate values (Al<sub>p</sub> and Fe<sub>p</sub> ranged from 0.02% to 1.06% and 0.02% to 1.51%, respectively, whereas the Al<sub>o</sub> and Fe<sub>o</sub> ranged from 0.03% to 2.52% and 0.03% to 2.13%, respectively). Exceptionally high values of Al<sub>o</sub> and Fe<sub>o</sub> were noted in profiles P1 and P2 (1.53% and 2.52% for Al<sub>o</sub>, and 2.13% and 1.46% for Fe<sub>o</sub>, respectively) in horizons Bs and BsC under *Plagiothecio-Piceetum tatricum*, as well as in horizon BsC of soils P10 and P13 (1.01% and 2.07% for Al<sub>o</sub>, and 1.33% and 1.31% for Fe<sub>o</sub>, respectively) located under the *Hieracio (vulgati)-Nardetum* (Table 3) plant community.

**Table 3.** Content of different forms of iron and aluminum and the values of indicators for spodic horizon in eluvial and illuvial soil horizon.

Profile Number	Soil Horizon	Al <sub>o</sub>	Fe <sub>o</sub>	Al <sub>p</sub>		Fe <sub>p</sub>		C <sub>p</sub>		Index of Al <sub>p</sub> , Fe <sub>p</sub> , C <sub>p</sub> Complex Content in Spodic Horizon	Molar Ratio of Organic Carbon to the Sum of Al <sub>p</sub> and Fe <sub>p</sub>	The Displacement Ratio of Amorphous Forms of Al <sub>o</sub> and Fe <sub>o</sub>
		%	%	%	mol	%	mol	%	mol			
1	AE	0.37	0.93	0.29	0.01	0.71	0.01	1.69	0.14	2.70	6.00	0.83
	Bs	1.24	2.13	0.77	0.03	1.51	0.03	3.28	0.27	5.55	4.93	2.31
	BC	1.53	0.92	0.83	0.03	0.84	0.02	2.58	0.21	4.26	4.67	2.00
2	A	0.30	0.43	0.21	0.01	0.25	0.00	1.85	0.15	2.31	12.53	0.51
	E	0.29	0.42	0.20	0.01	0.19	0.00	0.65	0.05	1.04	5.05	0.50
	BsC	2.52	1.46	1.06	0.04	0.96	0.02	1.98	0.17	4.01	2.92	3.25
3	AE	0.35	0.69	0.23	0.01	0.50	0.01	2.74	0.23	3.48	13.03	0.70
	BsC	0.75	1.03	0.56	0.02	0.65	0.01	2.54	0.21	3.75	6.55	1.27
	E	0.31	0.38	0.35	0.01	0.11	0.00	1.73	0.14	2.19	9.53	0.50
4	BsC	0.68	1.33	0.58	0.02	0.96	0.02	2.90	0.24	4.44	6.25	1.34
	AE	0.11	0.40	0.08	0.00	0.24	0.00	1.78	0.15	2.09	21.20	0.31
	E	0.41	0.08	0.04	0.00	0.07	0.00	0.84	0.07	0.94	26.28	0.45
5	BsC	0.54	0.89	0.38	0.01	0.66	0.01	2.02	0.17	3.06	6.50	0.98
	E	0.20	0.41	0.27	0.01	0.16	0.00	1.09	0.09	1.52	7.08	0.40
	BsC	0.90	1.28	0.37	0.01	0.86	0.02	2.08	0.17	3.31	5.93	1.54
6	E	0.23	0.17	0.17	0.01	0.13	0.00	1.12	0.09	1.42	10.74	0.31
	BsC	0.66	0.76	0.61	0.02	0.73	0.01	2.66	0.22	3.99	6.22	1.04
	AE	0.20	0.18	0.11	0.00	0.16	0.00	2.04	0.17	2.31	23.67	0.29
7	BsC1	0.29	0.42	0.10	0.00	0.17	0.00	1.65	0.14	1.92	20.13	0.50
	BsC2	0.93	1.77	0.40	0.01	1.03	0.02	2.37	0.20	3.80	5.91	1.82
	E	0.43	0.83	0.28	0.01	0.42	0.01	0.93	0.08	1.63	4.30	0.85
8	Bs	0.64	0.95	0.42	0.02	0.43	0.01	1.39	0.12	2.24	4.93	1.11
	BC	0.44	0.19	0.21	0.01	0.19	0.00	0.49	0.04	0.89	3.63	0.54
	AE	0.03	0.18	0.03	0.00	0.07	0.00	0.38	0.03	0.48	13.14	0.11
9	E	0.04	0.03	0.02	0.00	0.02	0.00	0.08	0.01	0.13	5.81	0.05
	BsC	1.01	1.33	0.65	0.02	0.92	0.02	1.39	0.12	2.96	2.84	1.68
	AE	0.36	0.36	0.30	0.01	0.27	0.00	1.69	0.14	2.25	8.91	0.55
10	BsC1	0.51	0.33	0.36	0.01	0.33	0.01	0.93	0.08	1.62	4.04	0.68
	BsC2	0.79	0.83	0.57	0.02	0.81	0.01	1.45	0.12	2.84	3.39	1.20
	A	0.21	0.54	0.11	0.00	0.30	0.01	1.04	0.09	1.46	9.17	0.48
11	AE	0.19	0.24	0.11	0.00	0.19	0.00	0.50	0.04	0.80	5.53	0.31
	BsC	0.60	1.36	0.42	0.02	0.87	0.02	2.02	0.17	3.31	5.39	1.28
	AE	0.91	0.82	0.64	0.02	0.38	0.01	1.97	0.16	3.00	5.36	1.32
12	BsC	2.07	1.31	1.00	0.04	0.94	0.02	1.99	0.17	3.92	3.07	2.73

Explanation: \* according to Mokma and Buurman [2]; \*\* according to WRB [40]; Al<sub>p</sub>, Fe<sub>p</sub>, C<sub>p</sub>—organically bound iron and aluminum extracted by a pyrophosphate solution; Al<sub>o</sub>, Fe<sub>o</sub>—“Active” iron and aluminum compounds extracted by an acid oxalate solution.

Based on the Al<sub>p</sub> and Fe<sub>p</sub>, as well as Al<sub>o</sub> and Fe<sub>o</sub> content, pedogenic (podzolization) indices were calculated. The values of podzolization indices varied, depending on the depth and type of vegetation cover. Index of Al<sub>p</sub>, Fe<sub>p</sub>, C<sub>p</sub> complex content in the spodic horizon ranged from 0.13% to 5.55%. The highest values were calculated in some soils under *Plagiothecio-Piceetum tatricum* (from 3.75% to 5.55% in spodic horizons). Relatively high values were also seen for soils P7 and P9, 2.24% and 3.99%, respectively (Table 3). The molar ratio of organic carbon to the sum of Al<sub>p</sub> and Fe<sub>p</sub> ranged from 2.84 to 26.2. It was clearly seen in the albic horizons that the values were higher comparing to the spodic horizon, which may indicate that more elements, including trace elements, were complexed by organic matter [48]. Analyzing the individual soil profiles, the values of this indicator were very diverse, depending on the vegetation cover. It was found that the highest values of the molar ratio of organic carbon to the sum of Al<sub>p</sub> and Fe<sub>p</sub> were noted partially in soils under *Vaccinium myrtillus*, e.g., soils P5 and P8 (26.28 and 23.67 mol, respectively).

The ratio of amorphous forms of Al and Fe ranged from 0.05% to 3.25%. The values were the highest in the spodic horizon and exceeded values higher than 0.5%, which is considered as one of the diagnostics for the spodic horizon [40] (Table 3). The highest values of podzolization index were characterized for soils P1 and P2 under *Plagiothecio-Piceetum tatricum* (2.31% and 3.25%, respectively) and soil P13 under *Hieracio (vulgati)-Nardetum*,

2.73%. In other soils, the values of this indicator in spodic horizons ranged from 0.54% (P9) to 1.82% (P8) (Table 3). In a view to above, each indicator showed the occurrence of the podzolization process in studied soils with different intensities.

### 3.5. Trace Element Content and Values of Pollution Indices

In some of the soil profiles, clear differences in accumulation with trace elements between the organic and mineral horizon were found (Table 4). Often, the highest values of trace elements were distinguished for organic horizons. Pb, Zn, and Cu had their highest contents especially in soils P2, P3, P4, P7, P10, and P11 (Table 4). The ranges of these elements in the O horizons differed, depending on the vegetation cover. The highest content of Zn, Cd, Cr, and Ni in organic horizons were determined in soils under *Hieracio (vulgati)–Nardetum* plant community, whereas the highest Pb and Cu contents were characteristic for organic horizons of soils under *Plagiothecio-Piceetum (tatricum)* and *Vaccinium myrtillus* vegetation cover, respectively. The occurrence of the highest values in the organic horizons was not a rule, since the highest values of trace elements were determined in lower horizons at times. In some soils, a decrease in the content of trace elements was observed in the E/AE horizon and then enrichment in the Bs/BsC horizon, which can be undoubtedly related to the podzolization process. Examples of soils where the visible depletion in the eluvial (E/AE) horizons and enrichment in the illuvial (Bs/BsC) horizons occurred as a result of the podzolization process were as follow: for Pb, Zn, Cu, Cr, and Ni—soils P2 and P12; for Zn, Cu, Cr, and Ni—soils P4 and P13; for Cd, Pb, and Zn—soil P3; for Cd and Pb—soils P1, P6, and P8; and finally, for Zn and Ni—soil P7 (Table 4, Figure 3a). The enrichment of illuvial horizon in trace element as the result of podzolization process on a smaller or larger scale have been observed in all studied soils (Table 5). The non-parametric Mann–Whitney U showed that there are differences in the content of trace elements between eluvial and illuvial horizons; however, it is statistically insignificant.

**Table 4.** Trace elements content in studied soils.

Profile	Horizon Symbol	Depth (cm)	Cd	Pb	Zn	Cr	Cu	Ni
1	Ol	0–10	1.38	24.8	26.8	9.55	9.73	3.33
	Oh	10–14	1.28	32.8	23.6	12.1	10.7	4.03
	AE	14–27	1.00	16.7	19.3	14.9	8.60	4.85
	Bs	27–44	1.03	19.7	33.5	22.4	11.5	8.95
	BC	44–56	0.75	17.5	49.3	26.2	13.6	17.0
2	Ol	0–4	1.33	49.3	45.3	15.2	14.4	4.25
	Oh	4–8	0.03	9.50	19.4	5.78	5.05	1.68
	A	8–18	2.03	16.5	19.0	5.10	5.83	1.63
	E	18–40	1.53	12.5	12.7	4.70	3.65	1.55
	BsC	40–70	0.38	19.4	34.8	14.1	6.03	5.13
3	Ol	0–4	0.23	11.5	21.2	5.93	5.63	2.00
	Oh	4–8	0.10	49.5	35.3	10.3	7.55	3.23
	AE	8–12	0.05	14.1	26.3	8.45	2.95	2.35
	BsC	12–28	1.53	20.8	11.8	3.28	1.13	0.95
4	Ol	0–2	1.15	34.3	38.3	6.85	8.00	2.53
	Oh	2–6	0.13	18.7	24.7	6.78	5.20	1.80
	A	6–14	0.20	11.2	13.3	3.80	2.15	0.75
	E	14–20	1.18	17.1	11.3	4.83	3.00	1.08
	BsC	20–39	1.33	18.0	24.2	9.00	3.38	2.00

Table 4. Cont.

Profile	Horizon Symbol	Depth (cm)	Cd	Pb	Zn	Cr	Cu	Ni
5	Olf	0–3	0.00	8.6	15.8	6.95	8.95	3.98
	A	3–7	0.20	11.7	15.6	9.10	9.73	4.68
	AE	7–19	1.50	17.7	11.1	11.2	5.70	3.53
	E	19–37	1.20	9.00	17.3	11.1	11.9	6.50
	BsC	37–50	1.43	16.6	16.5	13.1	12.0	8.00
6	Olf	0–6	0.60	13.8	44.3	4.33	8.20	2.83
	A	6–11	1.13	31.0	24.9	9.25	6.15	2.80
	E	11–16	0.93	10.7	44.8	12.4	5.08	2.58
	BsC	16–39	1.70	26.8	39.8	12.6	17.1	13.3
7	OI	0–3	0.73	34.3	41.3	13.2	13.3	3.65
	Oh	3–8	1.23	14.3	20.2	6.50	6.00	1.73
	A	8–23	0.28	4.90	13.7	3.15	1.83	0.85
	E	23–38	1.10	13.7	16.3	4.13	3.18	1.10
	BsC	38–58	0.90	11.7	25.5	3.65	1.70	1.58
8	Olf	0–10	1.05	44.8	49.3	9.63	13.9	4.55
	AE	10–33	0.40	13.4	34.5	12.7	25.7	10.5
	BsC1	33–40	1.28	20.1	44.8	18.3	35.0	13.2
	BsC2	40–60	1.60	28.0	65.8	19.7	35.5	14.7
9	Olf	0–6	0.30	19.5	60.8	27.7	14.3	12.6
	A	6–10	0.15	27.5	88.8	33.0	17.0	18.5
	E	10–18	1.45	26.0	71.3	42.7	15.5	15.2
	Bs	18–24	0.38	18.9	68.0	32.5	14.4	18.6
	BC	24–60	1.30	22.6	61.0	30.7	16.5	27.0
10	Olf	0–2	4.28	16.4	30.8	10.9	6.13	2.25
	A	2–6	0.08	10.0	24.6	14.3	5.95	2.53
	AE	6–23	1.08	12.8	12.1	6.43	1.35	1.40
	E	23–45	1.18	15.0	12.5	6.60	2.98	2.73
	BsC	45–70	0.20	14.2	72.3	24.9	6.85	12.5
11	Olf	0–3	0.38	37.3	42.5	7.85	10.5	3.60
	A	3–8	0.28	34.3	30.8	9.35	5.50	2.75
	AE	8–16	0.10	15.1	34.0	15.8	2.83	5.18
	BsC1	16–40	0.88	16.0	35.8	21.0	2.58	6.35
	BsC2	40–65	0.93	15.8	38.5	15.2	3.38	6.53
12	Olf	0–3	0.08	14.4	19.4	6.48	6.88	2.78
	A	3–26	0.08	9.80	14.7	4.13	3.78	2.00
	AE	26–43	0.08	4.50	14.6	4.90	4.68	2.18
	BsC	43–62	0.05	11.1	16.1	6.53	8.68	3.43
13	OI	0–3	1.23	25.3	43.3	12.4	12.0	4.50
	Oh1	3–6	0.18	33.3	43.8	14.0	10.6	5.08
	Oh2	6–20	1.48	32.8	31.3	12.4	5.45	3.78
	AE	20–50	0.20	19.1	30.0	12.0	6.25	4.48
	BsC	50–70	0.00	5.40	58.0	18.2	10.6	10.4

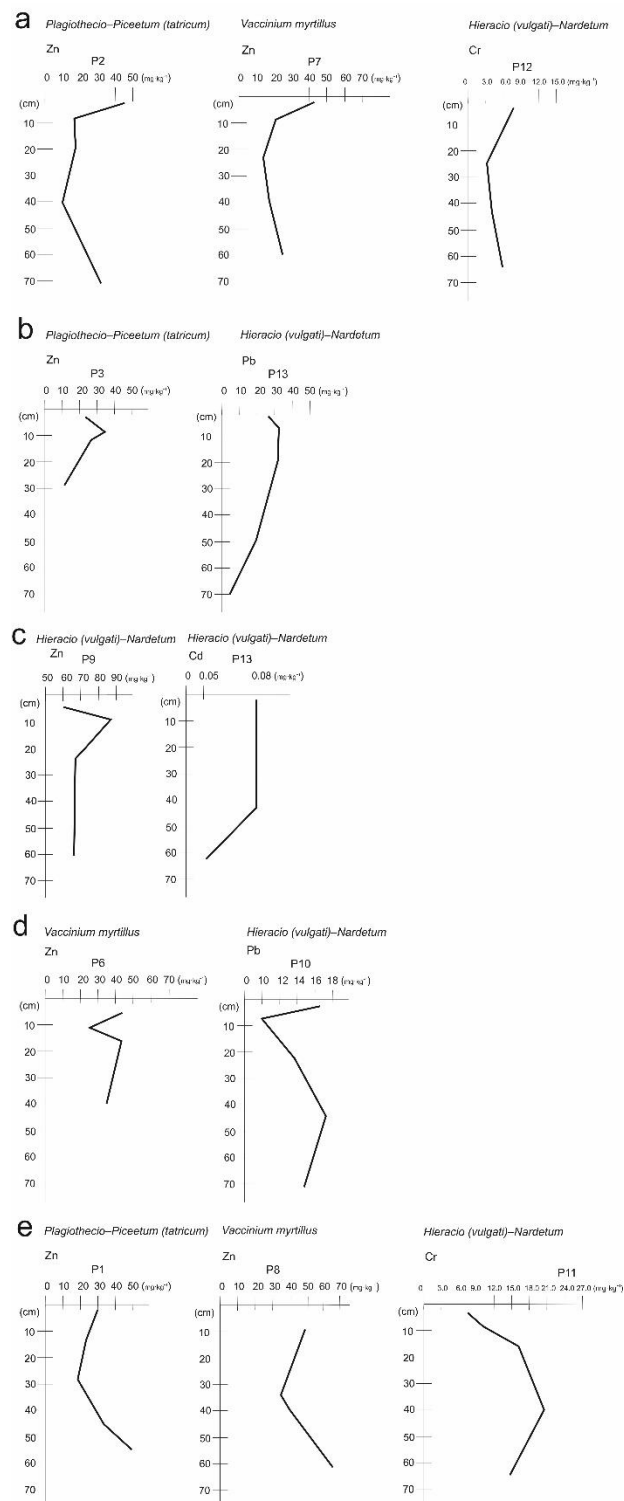


**Figure 3.** The examples of the various distribution of trace elements in soils under study. Explanation: (a) trace elements distribution as resulting from the podzolization process; (b) trace elements decreased with depth in the soil profile; (c) partially homogenous distribution of trace elements; (d) increasing of trace elements content in eluvial horizons, (e) enrichment with trace elements in BsC/BC horizon.

**Table 5.** The mean content of trace element in E and B horizons, standard error (the value in parentheses), and the U and *p* value estimated by the Mann–Whitney U test.

	E	B	U	<i>p</i>
Cd	0.80 (0.15)	0.85 (0.16)	81.50	0.898
Pb	14.38 (1.42)	16.82 (1.48)	54.00	0.124
Zn	26.53 (4.72)	37.01 (5.38)	54.50	0.130
Cr	11.96 (2.81)	15.38 (2.40)	58.00	0.182
Cu	7.42 (1.88)	10.09 (2.50)	70.00	0.473
Ni	4.64 (1.15)	8.05 (1.51)	55.00	0.137

In few cases, deviation from the expected distribution of trace elements as the result of the podzolization process occurred, which refer to depletion of eluvial horizon with trace elements and their accumulation in illuvial horizon. In some of the soil profiles, the content of trace elements simply decreased downward, e.g., soil P3 in the case of Pb, Zn, Cu, and Ni, and P13 in the case of Cd and Pb (Table 4, Figure 3b). Rarely, the content of trace elements was rather homogenous along the soil profile, e.g., soils P9 and P12 in the cases of Zn and Cd, respectively (Table 4, Figure 3c). It was often seen that the content of some trace elements was the highest in the eluvial horizon (E or AE). In soil P5, it was visible practically in case of all of the trace elements (Table 4, Figure 3d). Additionally, such a trend was found in, e.g., P6 (for Zn and Cr), P7 (for Cd, Pb, Cr, Cu), P9 (Cd), and P10 (Cd, Pb) (Table 4). Interestingly, strong enrichment with trace elements in the BsC/BC horizon occurred in soils P1 (for Zn, Cr, Cu, and Ni), P3 (Cd), P8 (Zn, Cr, Cu, and Ni), P10 (Zn, Cr, and Ni) and P11 (Cr); however, this was a result of the other factor than podzolization (Table 4, Figure 3e).

A very high content of Cd in the Olf horizon ( $4.28 \text{ mg}\cdot\text{kg}^{-1}$ ) occurred in soil P10, which could not be only the result of natural processes (Table 4). The highest value of Pb was characteristic for the Oh horizon of soil P3,  $49.5 \text{ mg}\cdot\text{kg}^{-1}$ . The highest contents of Zn were found in soils P8, P9, and P10 in BsC/BS horizons,  $65.8$ ,  $68.0$ , and  $72.30 \text{ mg}\cdot\text{kg}^{-1}$ , respectively (Table 4). Moreover, the A horizon of soil P9 showed a quite high content of Zn ( $88.8 \text{ mg}\cdot\text{kg}^{-1}$ ). Surprisingly, high values of Cr ( $22.4 \text{ mg}\cdot\text{kg}^{-1}$ ) were found in the Bs horizon of P1 and E horizon of P9 ( $42.7 \text{ mg}\cdot\text{kg}^{-1}$ ), suggesting not only the influence of the podzolization process for this element. The values of Cu in soil P8 in horizons BsC1 and BsC2 ( $35.0$  and  $35.5 \text{ mg}\cdot\text{kg}^{-1}$ , respectively) showed much higher concentrations than the other soils. The highest content of Ni ( $27.0 \text{ mg}\cdot\text{kg}^{-1}$ ) was determined in the BC horizon in soil P9, exceeding the content of Ni in the other studied soils (Table 4). The different origin of studied trace elements has been well visible on PCA diagram, where Cd evidently distinguish from other trace elements. Such components distribution on the diagram may suggested that Cd is the result of anthropogenic activity, whereas Pb, Zn, Cu, Ni, and Cr may come from natural sources, e.g., weathering of local parent substrates (Figure 4).

There were no particularly high differences in trace elements content in soils independent of the vegetation type. Considering the trace element values, in soils located under *Plagiothecio-Piceetum (tatricum)* (soils P1–4), only the content of Pb was the highest. In case of soils covered with *Vaccinium myrtillus* (soils P5–8), the highest content was detected in case of Cd, Cu, and Ni. Finally, the highest content of Zn and Cr was noted under *Hieracio (vulgati)–Nardetum* plant community (soils P9–13) (Table 1, Table 4).

The calculated pollution indices showed the potential degree of contamination of studied soils differed irrespective of the vegetation cover. According to  $I_{\text{geo}}$ , calculated for Cd, the soils were unpolluted to moderately polluted (Figure 5a). Some of the horizons showed moderate pollution, which applied only to certain horizons of soils P2–P6, P8, and P9. Additionally, the Olf horizon of soil P10 was highly polluted (Figure 5a). Furthermore, the  $I_{\text{geo}}$  calculated for Pb, Cr, Zr, and Ni showed a predominance of unpolluted to moderately polluted soil samples (Figure 5a), whereas, in case of Cu, soils were unpolluted to moderately polluted. Moderate to high pollution was noted in soil P8 in case of Cu content (Figure 5a).

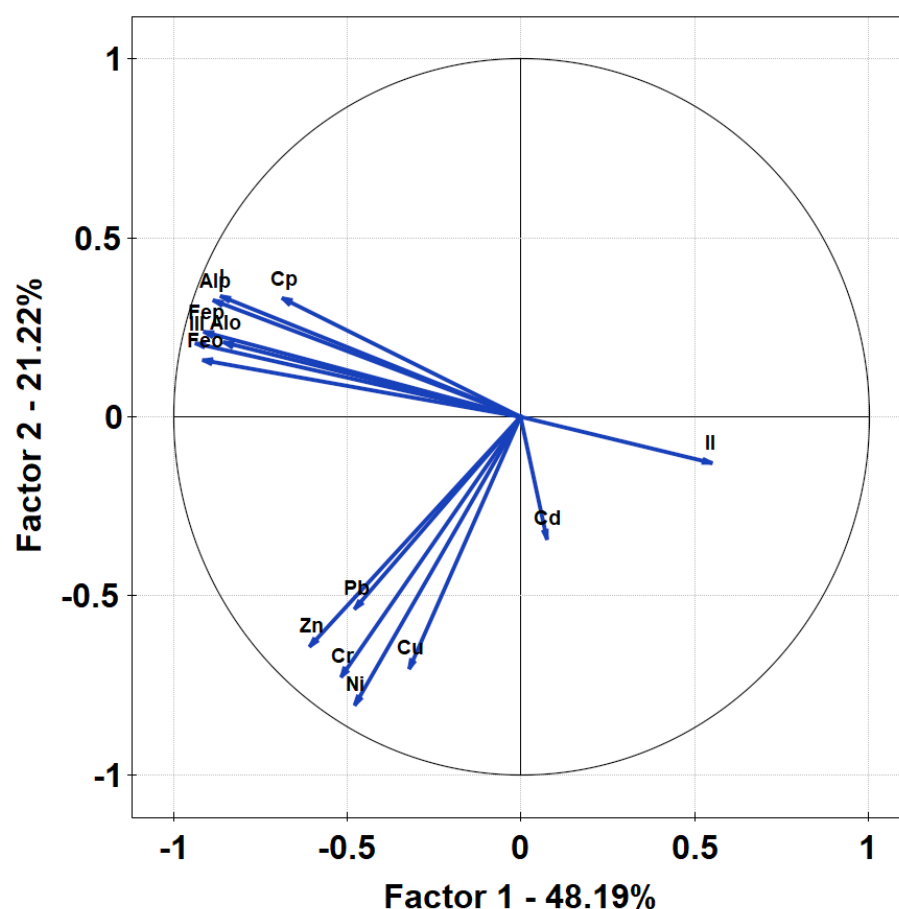


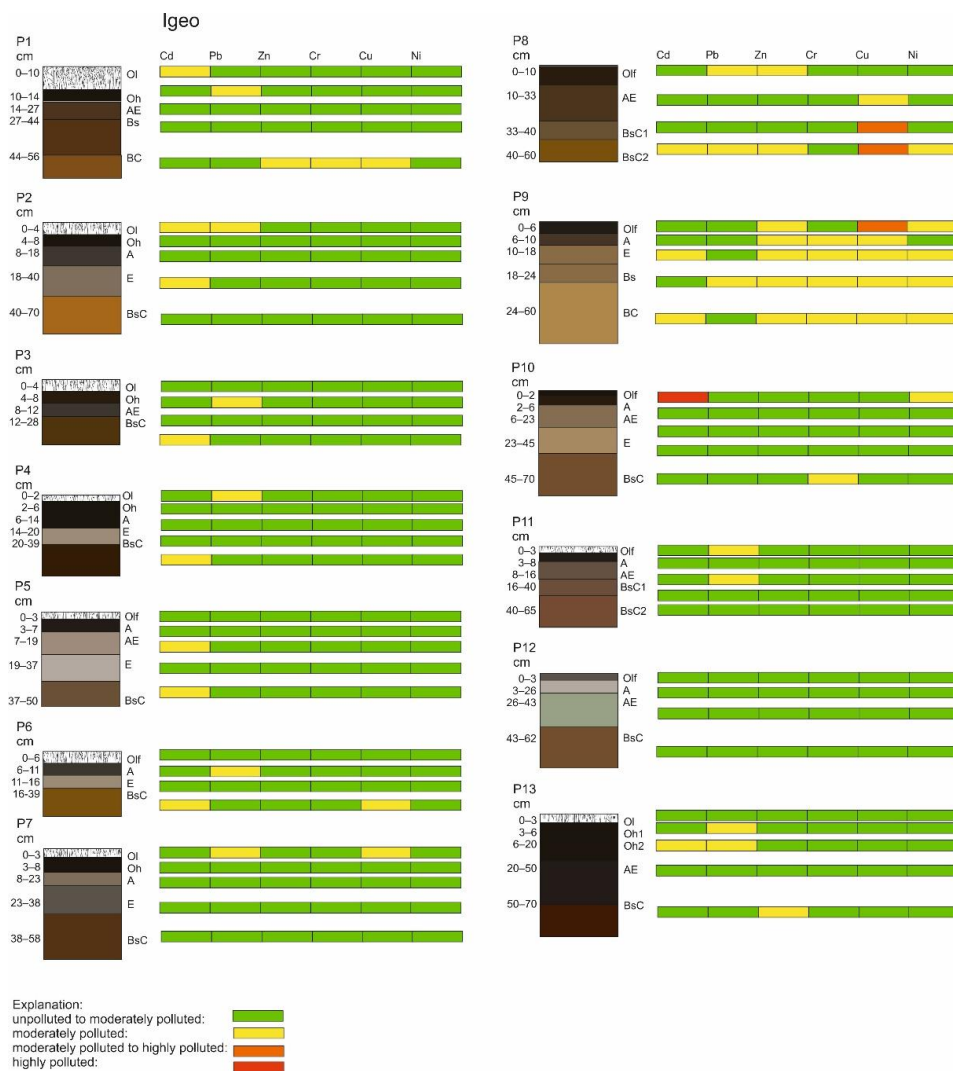
**Figure 4.** Principal components analysis (PCA) of trace elements contents, pedogenic indices, and various forms of Al and Fe. Explanation: Al<sub>p</sub>, Fe<sub>p</sub>, C<sub>p</sub>—“organically bond” forms of Al and Fe extracted with pyrophosphate solution; Al<sub>o</sub>, Fe<sub>o</sub>—“active” forms of Al and Fe extracted with acid oxalate solution; I—index of Al<sub>p</sub>, Fe<sub>p</sub>, C<sub>p</sub> complex content in spodic horizon; II—molar ratio of organic carbon to the sum of Al<sub>p</sub> and Fe<sub>p</sub>; C<sub>p</sub>/Al<sub>p</sub> + Fe<sub>p</sub>, III—the displacement ratio of amorphous forms of Al<sub>o</sub> and Fe<sub>o</sub>.

RI values confirm low potential ecological risk. Only in soil, P10 has a moderate stage of this index in the organic horizon (Figure 5b). According to the PLI values, most of the studied soils were categorized as high quality, while some of the soils showed some deterioration of soil quality (partially soils P1, P5, P6, and P8, and completely soil P9; Figure 5b). CSI values indicated that soils were characterized by a low pollution severity. However, some of the soils were uncontaminated, e.g., soil P12 (Figure 5b).

#### 4. Discussion

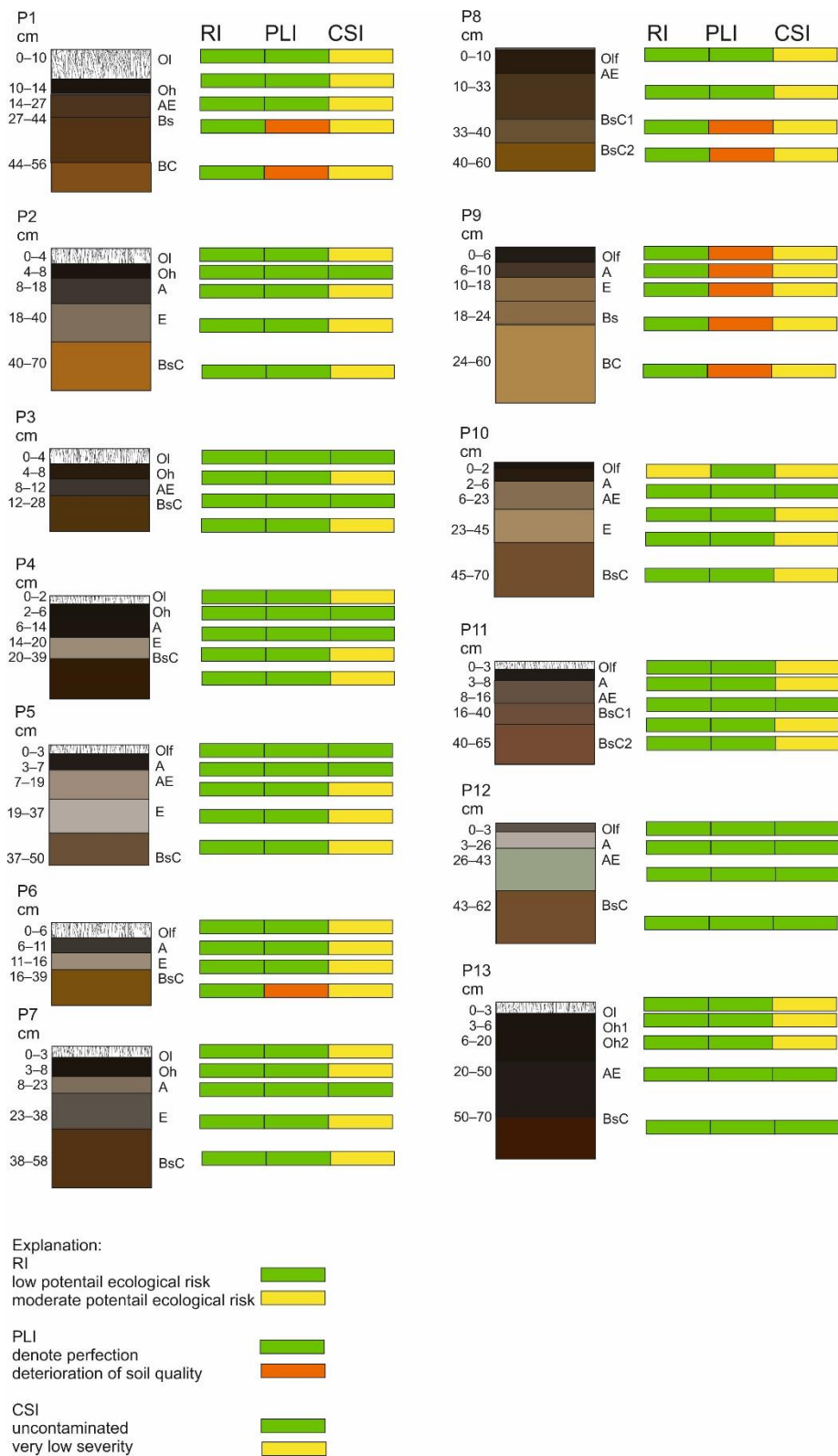
In the studied soils, the evident translocation of various forms of Fe and Al, which is typical for podzolization process [49–51], was confirmed by three indicators. First, the podzolization index ( $Al_o + 0.5 Fe_o$ ) exceeded values higher than 0.5% (Table 3), indicating the clear development of a spodic horizon [40]. These features correspond with requirements of World Reference Base for Soil Resources [40], allowing these soils to be classified as Podzols (Table 1). Furthermore, the molar ratio of organic carbon to the sum of Al<sub>p</sub> and Fe<sub>p</sub> ( $C_p / Al_p + Fe_p$ ), met the requirements for spodic horizon given by Mokma and Buurman [2], which have to be with a range of 5.8 to 30 (Table 3). Statistically, the podzolization indices did not indicated significant difference in terms of rates of this process itself (Figure 4); however, all of them confirmed the occurrence of this process in studied soils.

The podzolization process in studied soils is supposed to be strongly connected with vegetation cover [1,9,10,14,52]. However, the pedogenic indices did not point unequivocally under which plant habitats the podzolization process was more advanced. Highest values of podzolization index as well as Al and Fe extracted with pyrophosphate solution (Table 3) were found in the soils under *Plagiothecio-Piceetum (tatricum)*. This finding is in good agreement with data of Nikodem et al. [9] who stated that podzolization intensity is higher under coniferous forest. Similarly, Zwanzig et al. [15] reported that the podzolization process is more intensive under coniferous forest or coniferous-mixed than under grass-herb cover or deciduous vegetation. Moreover, Lundström et al. [1] noted that Podzols development may be favored by coniferous and ericaceous shrubs; thus, also other advantageous vegetation conditions might lead to increased podzolization. Of course, we should keep in mind that the vegetation cover in the Tatra Mts. change over the decades and hundreds of years. For instance, vast areas where *Hieracio (vulgati)-Nardetum* and *Vaccinium myrtillus* are common nowadays, have been overgrown by coniferous forest in the past, and there were (at least partially) either spruce or ecotone communities present, which favored podzolization [9,53].



(a)

Figure 5. Cont.



(b)

**Figure 5.** The interpretation of pollution indices values: (a) Matrix of Geoaccumulation Index ( $I_{geo}$ ) values in studied soils. The interpretation of pollution indices values: (b) Potential Ecological Risk (RI), Pollution Load Index (PLI) and Contamination Security Index (CSI) values calculated on the basis of studied trace elements.

The trace element distribution in studied soils should indicate the pattern typical for Podzols, clear peak of trace elements accumulation in B horizons. Nonetheless, the studied shallow mountain Podzols did not always show this trend so clearly, mostly because these horizons represent the deepest (BsC horizon) (Table A1). Thus, in such situations, it is difficult to estimate the exact point (horizon) where the enrichment of trace elements occurred as a direct result of podzolization. However, considering the site-specificity of mountain soils, high abundances of rock fragments and dense soil horizons cause limitations to percolation [1,4]; these may be a possible factors that hamper maximum depth of podzolization [54]. Consequently, trace elements in the BsC horizons of the studied soils should indicate the maxima related to the podzolization process itself [48].

Analyzing the trace element arrangements in studied soils, it can be noted that, in most profiles, podzolization influenced the accumulation of Pb, Zn, Ni, and less Cr (Table 5) in the Bs and/or BsC horizons that met the criteria for a spodic horizon. In those profiles, the effect of the trace elements distribution is rather undisturbed, and their deep storage occurs as a result of podzolization (Table 4) [1,55]. Although, the difference between the content of trace elements in eluvial and illuvial horizons according the Mann–Whitney was statistically insignificant ( $p > 0.05$ ), it was the tendency, especially the case of Pb, Zn, Ni, and less Cr, their higher content in the illuvial horizon (Table 5). This may suggest the deep storage of these elements. However, we should keep in mind that their high contents in the subsoil might also be an effect of local lithology (e.g., Figure 3e). This is especially a case issue in soils developed from slope deposits where we expect multiple sources of trace elements, e.g., in the lowermost horizons, not related to podzolization.

Nonetheless, the studied Podzols also showed other patterns of the trace elements distribution, which for the purposes of this work were called “anomalies”, and represent deviations from the general trend triggered by podzolization process. Anomalies in studied soils were distinguished with regard to the distribution of trace elements that should be present in the podzolization process. In the traditional arrangement within Podzols profiles, two maximum values of trace elements concentration should be observed—in the O horizon, where natural bioaccumulation occurs, and in Bs horizon, where the enrichment with trace elements may be expected due to translocation [4,16]. Where the content of trace elements in the Bs horizon exceeds the maximum content of trace elements in the O horizons, this means that the effect of podzolization itself cannot be longer considered.

However, because the content of trace elements is much higher in the BsC horizon compared to the upper O horizons, it is rather doubtful that the entire pool of trace elements was leached and accumulated in the illuvial horizon. The trace elements probably have not been washed out entirely, and their displacement from Olf/ Oh into Bs horizons was not related with podzolization only. It thus seems right to conclude that it is not the pedogenic factors, but the lithological factors that have a greater effect on soil enrichment with trace elements [56,57]. It is reasonable to state that at least partially the source of trace elements in BsC horizon consists of the parent rock with varying degrees of weathering or representing sudden changes of lithology [58,59].

The parent material of the studied Podzols, e.g., Pleistocene moraine deposits, granite gneisses and sandstone slope deposits, could be reworked by a glacier [60]. Such mixed deposits, with different degree of weathering, could be the main cause for the presence of geochemical anomalies reflected in specific trace elements distribution, not connected with podzolization. However, the input of trace elements coming from weathering of the lowermost soil horizons and those being translocated due to podzolization is hard to measure [57], especially in case of low concentration of trace elements in topsoil compared with the subsoil (BC horizons). Such anomalies were present in soils under each of vegetation types, e.g., Zn content in soil P1 (*Plagiothecio-Piceetum (tatricum)*), and soil P8 (*Vaccinium myrtillus*), Cr content in case of soil P11 (*Hieracio (vulgati)–Nardetum*, Figure 3e, Table 4)

The studied soil represents also other unusual trends of trace elements. Besides the two main trends, such as (i) traditional distribution resulting from the podzolization process (Figure 3a), and the (ii) enrichment of Bs/BsC horizons due to parent material

weathering (Figure 3e), three additional cases could be considered in this study. Some of the soils reveal (iii) decrease of the content of trace elements with soil depth (Figure 3b), (iv) quite homogenous distribution of trace elements (Figure 3c), and (v) enrichment in E horizon (Figure 3d). As far as (iii) is concerned, the decrease of trace elements down the soil profile (Figure 3b) is quite common, especially due to bioaccumulation or when the high accumulation of trace elements in the surface horizons is considered as the result of the anthropogenic activity [27,29].

The other above-mentioned cases—homogenous distribution and enrichment of trace elements in the E horizon—could be related mostly with the erosion and translocation processes of soil material, since this could disturb their natural accumulation in Bs/BsC horizon. These results are consistent with the data in Zhu et al. [61], where the relationship between topography and the distribution of some trace elements in the soil profile was noted. Similarly, according to Henkner et al. [62], slope erosion triggered redistribution of trace elements what is well visible in those two cases of anomalies as mentioned above (Figure 3c,d).

It was reported that the effect of podzolization on trace elements distribution may be additionally controlled by plant communities [63,64]. Generally, the greater potential for the transfer of Fe/Al-organic complexes and more decomposed organic matter in the soil, the easier translocation of trace elements down the soil profile [64,65]. Simultaneously, sites with coniferous forests should be less enriched by trace elements than grass and blueberry habitats, because one, they decompose more slowly and two, with a cover made by upper branches of a coniferous tree they can constitute a natural protective barrier.

Thus, in view of the above, the studied soils developed under *Hieracio (vulgati)*–*Nardetum* and *Vaccinium myrtillus* ecosystems should reveal a higher accumulation potential of trace elements in the spodic horizon, since the organic debris from these plant communities can degrade faster than, for example, coniferous forests [63]. However, in this study, no direct relationship was found between the vegetation type and trace elements translocation. Similar results were obtained by MacDonald and Hendershot [57] in a study over Podzols in northern forest ecosystems (Rouyn-Noranda, Canada). The accumulation of trace elements in all of the studied soils has more or less the same intensity in the Bs/BsC horizons, which was also well visible on “whisker plot” (Figure 6) diagrams for Zn, Pb, Cd, showing large spreads between the minimum and maximum values and the median (Figure 6). However, the “whisker plot” for Pb of Bs horizons of soils under *Vaccinium myrtillus* (Figure 6) showed a different relationship—the spread was lower compared to other habitats—but this could be influenced rather by very local conditions, e.g., microrelief or the deposition of Pb from the atmosphere [19].

On the other hand, Zn unexpectedly showed the greatest accumulation in the spodic horizon in soils under the coniferous forest (Table 4). This can be related to the possible change in the vegetation cover resulting from the gradual disappearance of coniferous forests over the years [52]. Because of this, the inflow of substances acidifying the soil as well as leaching within the solum could have stopped [66]. The remained litter can be overgrown, by, e.g., grass and shrubs, and often favors an increase in trophic index through that returning more calcium, magnesium, nitrogen into the soil that further is subjected to accelerated mineralization [66]. As a result, the trace elements can be theoretically activated and able to percolate into the lowermost soil horizons [48,57].

Moreover, the highest content of trace elements was observed in the organic horizon (Table 4) regardless of the plant habitat [63,64,67]. This is not unexpected, since trace elements are prone to strong accumulation in litter [67]. In this study, in the case of *Vaccinium myrtillus*, it can be seen that with increasing altitude, the content of trace elements in O horizons was also higher, see, e.g., Zn, which may be influenced by the deposition from external factors and have at least traces of some anthropogenic activity [30,67]. Similarly, the content of Cd in O<sub>1</sub> horizon of P10 also might suggest anthropogenic input, since very high values were noted (4.28 mg·kg<sup>−1</sup>, Table 4). The anthropogenic origin of Cd was also visible on PCA diagram (Figure 4). It was noticeable that Cd arranged in a

completely different part of the chart, what is in good agreement with the assumption that it has a different origin than another studied trace elements (Figure 4). Considering such high values, the wet deposition of trace elements from long-distance transport seems reasonable [20,68].

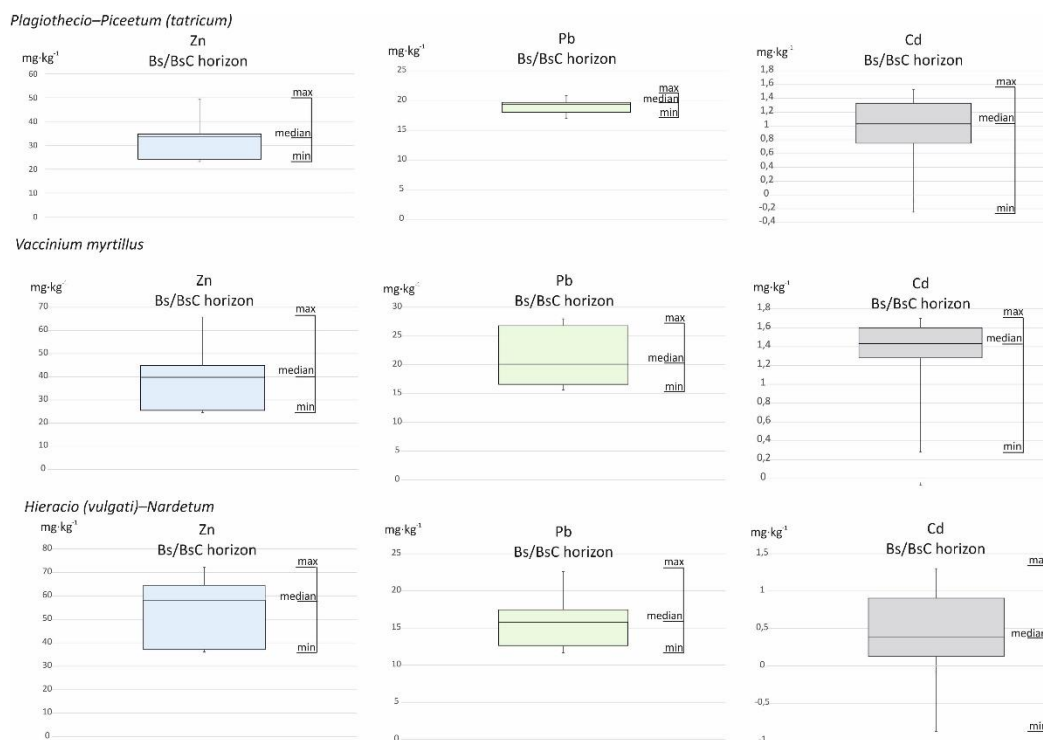


Figure 6. Whisker plots diagram on Zn, Pb, and Cd content in Bs or BsC horizon in soils under various vegetation types.

Many authors have noted that mountain areas are susceptible to retaining pollution, often containing trace elements [16,19,69,70]. The Tatra Mts. are exposed to airborne pollution from the local and the distant sources, thus it was assumed that the studied soils could hold higher contamination levels [17,18,71]. For example, studies of Miechówka et al. [18] showed an excessive concentration of Cd, Pb, and also Cr and Zn in non-forest soils from TPN. Similarly, Grodzińska et al. [72] also reported that the TPN had one of the highest levels of pollution with Cd, Cr, Ni, Pb, Cu, and Zn among the Polish National Parks.

However, when analyzing the content of trace elements, pollution cannot be clearly demonstrated. The values of trace elements were rather low when considering potential contamination and only showed differences between individual soil horizons (Table 4). Based on that, it seems that Tatra Mts. is unaffected by pollutants compared to other selected areas of mountainous and upland National Parks in Poland, e.g., Ojców National Park, Babia Góra National Park, Pieniny National Park, Karkonosze National Park, Roztocze National Park [20,30,72,73]. Furthermore, also analyzing other data concerning the mountainous areas, from, e.g., Ghazaryan et al. [74], the studied soils indicated very natural ranges of values.

To analyze the potential pollution of studied soils more comprehensively, a set of pollution indices was calculated, which could indicate even the smallest potential ecological risk and allow the determination of the cause of possible enrichment with trace elements [27,28]. The indicators, except a few horizons marked as yellow, orange, and/or red (Figure 5a,b), confirmed that the studied soils were not contaminated (Figure 5a,b).

Based on  $I_{geo}$  and PLI, only soils P8 and P9 showed pollution, however locally (Figure 5a), especially with Cu (P8 and P9) and Zn (P9), but it is the result of inheritance of trace elements from parent material and cannot be strictly connected to anthropogenic activity [28]. The RI did not indicate any potential ecological risk, whereas only the CSI values

suggested low severity (Figure 5b) [28]. Quite similar results were shown by Stobiński and Kubica [71], who noted that the soils of five major valleys of the Polish part of the Tatra Mts. (Chochołowska, Kościeliska, Suche Wody, Rybiego Potoku, and Bystra Valleys) indicated the incidental occurrence of high concentrations of trace elements and stated mainly a natural origin for any enrichment. However, the obtained data are in contradiction with Mazurek et al. [20,30], Pacyna and Pacyna [75], and Steinnes et al. [76], who reported that even soils located far from direct emission sources can be strongly contaminated as the result of anthropogenic activity. Nonetheless, such low values of trace elements in the studied soils may be an effect of research site localizations. Perhaps the soil profiles were located within a topographic (mountainous) barrier, below the main ridge in an isolated position on the slope, that protects the studied area, and trace elements-rich pollution could not reach and accumulate on the surface of the studied soils [19,30].

Contrariwise, the pollution indices themselves may not be suitable for Podzols, where the translocation of trace elements via podzolization into deeper soil horizons additionally raises trace element content. This could be an impediment both for geochemical background calculation but also for pollution indexes estimation. Therefore, the calculated pollution indices could not always give the appropriate values. By the fact that the expected deep storage in the studied soils occurs very locally (Figure 3a,e), a significant role in the heterogeneous distribution of trace elements is played rather by the differentiation of the parent substrate and the anomalies discussed above—abrupt decreases and increases of trace elements contents, not related to the prevailing soil process (Figure 3e). It should be noted that Podzols require a specific approach and, above all, specific diagnosis on potential trace elements contamination. However, there are no other reports in the literature indicating that in case of soils under podzolization, the application of pollution indices may misinterpret the degree of pollution. Moreover, based on the obtained total content of trace elements, as their values are rather low and did not suggest pollution, the values of the calculated pollution indices (Figure 5a,b) seemed to be reasonable.

Yet, pollution indices did not show variation in trace elements content in soil under different vegetation cover. No trend was visible, suggesting that the contamination degree could be potentially higher under a specific vegetation cover (Figure 5a,b). The obtained pollution indices data mostly suggested a similar degree of pollution. Only soil P1 under *Plagiothecio-Piceetum (tatricum)* and P9 under *Hieracio (vulgati)–Nardetum* were distinguished from the rest of the studied Podzols (Figure 5a,b); nonetheless, this did not uniquely determine any relationship between indices of pollution and different type of vegetation cover.

## 5. Conclusions

The podzolization process was mostly connected with vegetation cover. Based on this, coniferous forests had the greatest influence on the formation of Podzols in the study area. The podzolization process in studied soils determined the translocation of trace elements from uppermost horizons into the illuvial horizon, but yet, only locally. It was quite visible through the distribution of Pb, Zn, Ni, and Cr in some soils by the accumulation in the Bs and/or BsC horizons that met the criteria for the spodic horizon. The accumulation of trace elements in the Bs and/or BsC horizons as an effect of undisturbed podzolization may lead to their deep storage in the spodic horizon. Yet, the pattern of trace element distribution typical for podzolization may be disturbed by different lithologies, and then anomalies in trace element distribution might appear. Anomalies were characterized by a much higher content of trace elements in the BsC horizon compared to the upper O horizons. The occurrence of such anomalies in some of the studied soils resulted not only from the podzolization process, but also mainly from the enrichment of Bs and/or BsC horizon through heterogeneous parent material and its weathering. Such anomalies were visible in soils under all studied vegetation types. Only the Zn content showed its highest accumulation in the spodic horizon in soils under coniferous forests. Nonetheless,

regardless of the plant habitat, most of the trace elements accumulated in the O horizon, may be as the result of deposition of trace elements from long-distance transport.

The content of trace elements in the studied soils was rather low; thus, the presence of pollution cannot be clearly stated. The pollution indices also suggested the lack of contamination in the majority of soils, which could result from locations outside the main deposition air patterns for trace elements-rich pollutants. On the other hand, pollution indices might not give an appropriate value in the case of soils under podzolization process. However, the results of pollution indices seem to be correct, since the raw data of trace element concentrations and profile locations did not indicate the presence of contamination either.

**Author Contributions:** Conceptualization, J.B.K., J.W., and M.G.; methodology, J.B.K., P.Z., and M.G.; formal analysis, P.Z. and P.N.; investigation, P.Z. and P.N.; resources, J.B.K. and P.Z.; data curation, J.B.K. and P.Z.; writing—original draft preparation, J.B.K.; writing—review and editing, J.B.K.; J.W., and M.G.; visualization, J.B.K.; supervision, J.B.K. and J.W.; project administration, J.B.K. All authors have read and agreed to the published version of the manuscript.

**Funding:** This research received no external funding.

**Conflicts of Interest:** The authors declare no conflict of interest.

## Appendix A

**Table A1.** Morphological characteristics of the studied soils.

Profile Number	Soil Horizon	Depth (cm)	Colour *	Boundary	Structure	Consistence (Moist)	Coarse Fragments (%)	Moisture	Abundance of Roots
1	Ol	0–10	n.d.	A	n.d.	n.d.	n.d.	M	M
	Oh	10–14	10 YR 1.7/1	A	n.d.	FR	n.d.	M	F
	AE	14–27	7.5 YR 3/3	A	ME SB MO	FI	C	M	F
	Bs	27–44	7.5 YR 3/4	C	FI SB MO	VFI	M	M	V
	BC	44–56	7.5 YR 4/6	-	FI SB MO	VFI	A	M	V
2	Ol	0–4	n.d.	A	n.d.	n.d.	n.d.	M	M
	Oh	4–8	10 YR 1.7/1	C	n.d.	FR	n.d.	M	C
	A	8–18	7.5 YR 3/1	C	FI SB WE	FR	M	M	F
	E	18–40	10 YR 5/2	C	VF SB WE	FI	A	M	V
	BsC	40–70	7.5 YR 5/8	-	SG	VFI	A	M	N
3	Ol	0–4	n.d.	A	n.d.	n.d.	n.d.	M	M
	Oh	4–8	10 YR 2/2	A	n.d.	FR	n.d.	M	M
	AE	8–12	10 YR 3/1	A	FI GR MO	FI	A	M	C
	BsC	12–28	7.5 YR 3/4	-	FI GR WE	VFI	D	M	V
4	Ol	0–2	n.d.	A	n.d.	n.d.	n.d.	M	M
	Oh	2–6	10 YR 1.7/1	A	n.d.	FR	n.d.	M	M
	A	6–14	10 YR 1.7/1	C	FI SB WE	FR	n.d.	M	C
	E	14–20	10 YR 6/2	A	FI SB MO	FI	A	M	F
	BsC	20–39	7.5 YR 2/3	-	FI SB MO	VFI	A	M	F
5	Olf	0–3	n.d.	A	n.d.	n.d.	n.d.	M	M
	A	3–7	7.5 YR 2/1	C	VF CR WE	FR	C	M	M
	AE	7–19	7.5 YR 6/2	G	FI GR WE	FI	M	M	F
	E	19–37	7.5 YR 7/1	C	FI GR MO	FI	A	M	V
	BsC	37–50	7.5 YR 4/3	-	FI GR MO	VFI	D	M	N
6	Olf	0–6	n.d.	A	n.d.	n.d.	n.d.	M	M
	A	6–11	10 YR 3/1	A	VF CR WE	FR	n.d.	M	F
	E	11–16	10 YR 6/1–2	A	VF CR MO	FI	M	M	V
	BsC	16–39	10 YR 4/6	-	SG	VFI	A	SM	N
7	Ol	0–3	n.d.	A	n.d.	n.d.	n.d.	M	M
	Oh	3–8	10 YR 1.7/1	C	n.d.	FR	n.d.	M	F
	A	8–23	10 YR 5/2	A	FI SB ST	FI	n.d.	M	F
	E	23–38	10 YR 4/1	A	FI SB ST	FI	C	M	V
	BsC	38–58	7.5 YR 3/4	-	FI SB MO	VFI	M	M	V

Table A1. Cont.

Profile Number	Soil Horizon	Depth (cm)	Colour *	Boundary	Structure	Consistence (Moist)	Coarse Fragments (%)	Moisture	Abundance of Roots
8	Olf	0–10	10 YR 2/2	A	n.d.	FR	n.d.	M	M
	AE	10–33	10 YR 3/3	C	VF GR WE	FI	C	M	F
	BsC1	33–40	10 YR 4/3	C	SG	VFI	M	M	F
	BsC2	40–60	10 YR 4/6	-	SG	VFI	A	M	V
9	Olf	0–6	10 YR 2/1	A	n.d.	FR	n.d.	M	M
	A	6–10	7.5 YR 3/2	A	FI AB MO	FR	M	M	F
	E	10–18	10 YR 5/4	A	FI AB MO	FI	M	M	F
	Bs	18–24	10 YR 5/3	A	FI AB MO	VFI	A	M	F
	BC	24–60	10 YR 6/6	-	FI SB MO	VFI	A	M	V
10	Olf	0–2	10 YR 1.7/1	A	n.d.	n.d.	n.d.	M	M
	A	2–6	10 YR 2/2	C	SG	FR	F	M	M
	AE	6–23	10 YR 5/3	C	VF CR MO	FI	M	M	F
	E	23–45	10 YR 6/3-4	C	VF CR WE	FI	A	M	F
	BsC	45–70	7.5 YR 4/4	-	SG	VFI	A	M	V
11	Olf	0–3	n.d.	A	n.d.	n.d.	n.d.	M	M
	A	3–8	10 YR 2/1	A	VF CR MO	FR	n.d.	M	C
	AE	8–16	7.5 YR 4/2	C	FI SB MO	FI	n.d.	M	F
	BsC1	16–40	5YR 4/3	G	FI SB MO	VFI	M	M	F
	BsC2	40–65	5 YR 4-3/4	-	FI SB MO	VFI	A	M	F
12	Olf	0–3	7.5 YR 4/1	C	n.d.	FR	n.d.	M	M
	A	3–26	7.5 YR 7/1	C	SG	FR	M	M	C
	AE	26–43	7.5 YR 6/1	A	FI GR MO	FI	A	M	F
	BsC	43–62	7.5 YR 4/4	-	FI AB WE	VFI	A	M	V
13	Ol	0–3	n.d.	A	n.d.	n.d.	n.d.	M	M
	Oh1	3–6	10 YR 1.7/1	C	n.d.	FR	n.d.	M	M
	Oh2	6–20	10 YR 1.7/1	C	n.d.	FR	M	M	C
	AE	20–50	7.5 YR 2/1	A	FI AB MO	FI	A	M	F
	BsC	50–70	5 YR 2/4	-	FI AB MO	VFI	D	M	V

Explanation: \* according to Munsell Color Charts (1975); boundary (FAO, 2006): distinctness: A—abrupt; C—clear; G—gradual; structure (FAO, 2006): (1) size classes: VF—very fine; FI—fine; ME—medium. (2) Types of structure: CR—crumby; GR—granular; AB—angular blocky; SB—subangular blocky. (3) Classification of structure: WE—weak; MO—moderate; ST—strong. Consistence (FAO, 2006): FR—friable; FI—firm; VFI—very firm. Abundance of rock fragments by volume (FAO, 2006): C—common; M—many; A—abundant; D—dominant. Moisture (FAO, 2006): SM—slightly moist; M—moist. Abundance of roots (FAO, 2006): N—none; V—very few; F—few; C—common; M—many; n.d.—not determined.

## Appendix B

Table A2. Particle size distribution of studied soils.

Profile Number	Soil Horizon	Depth (cm)	Particle Size Distribution (%)								Texture Group
			2.0–1.0 mm	1.0–0.5 mm	0.5–0.250 mm	0.25–0.1 mm	0.1–0.05 mm	0.05–0.02 mm	0.02–0.005 mm	<0.002 mm	
1	Ol	0–10	n.d.	n.d.	n.d.	n.d.	n.d.	n.d.	n.d.	n.d.	n.d.
	Oh	10–14	n.d.	n.d.	n.d.	n.d.	n.d.	n.d.	n.d.	n.d.	n.d.
	AE	14–27	18	4	13	5	12	19	20	9	SL
	Bs	27–44	34	1	23	4	11	18	6	3	LS
	BC	44–56	25	24	21	1	8	9	10	2	LS
2	Ol	0–4	n.d.	n.d.	n.d.	n.d.	n.d.	n.d.	n.d.	n.d.	n.d.
	Oh	4–8	n.d.	n.d.	n.d.	n.d.	n.d.	n.d.	n.d.	n.d.	n.d.
	A	8–18	34	12	1	9	14	12	10	8	SL
	E	18–40	23	10	10	12	8	12	17	8	SL
	BsC	40–70	33	27	3	14	12	7	4	0	S
3	Ol	0–4	n.d.	n.d.	n.d.	n.d.	n.d.	n.d.	n.d.	n.d.	n.d.
	Oh	4–8	n.d.	n.d.	n.d.	n.d.	n.d.	n.d.	n.d.	n.d.	n.d.
	AE	8–12	45	12	3	5	16	7	5	7	LS
	BsC	12–28	39	13	3	4	12	12	11	6	SL

Table A2. Cont.

Profile Number	Soil Horizon	Depth (cm)	Particle Size Distribution (%)								Texture Group	
			2.0–1.0 mm	1.0–0.5 mm	0.5–0.250 mm	0.25–0.1 mm	0.1–0.05 mm	0.05–0.02 mm	0.02–0.005 mm	<0.002 mm		
4	Ol	0–2	n.d.	n.d.	n.d.	n.d.	n.d.	n.d.	n.d.	n.d.	n.d.	n.d.
	Oh	2–6	n.d.	n.d.	n.d.	n.d.	n.d.	n.d.	n.d.	n.d.	n.d.	n.d.
	A	6–14	n.d.	n.d.	n.d.	n.d.	n.d.	n.d.	n.d.	n.d.	n.d.	n.d.
	E	14–20	35	13	1	2	12	23	11	3	SL	
	BsC	20–39	46	1	23	1	9	10	9	1	LS	
5	Olf	0–3	n.d.	n.d.	n.d.	n.d.	n.d.	n.d.	n.d.	n.d.	n.d.	n.d.
	A	3–7	43	17	5	6	10	10	4	5	LS	
	AE	7–19	38	18	1	1	17	10	10	5	LS	
	E	19–37	47	9	1	2	8	7	18	8	SL	
	BsC	37–50	42	13	2	8	11	7	11	6	SL	
6	Olf	0–6	n.d.	n.d.	n.d.	n.d.	n.o.	n.o.	n.d.	n.d.	n.d.	n.d.
	A	6–11	n.d.	n.d.	n.d.	n.d.	n.o.	n.o.	n.d.	n.d.	n.d.	n.d.
	E	11–16	48	2	17	7	13	7	6	0	LS	
	BsC	16–39	56	15	13	0	9	4	3	0	S	
7	Ol	0–3	n.d.	n.d.	n.d.	n.d.	n.d.	n.d.	n.d.	n.d.	n.d.	n.d.
	Oh	3–8	n.d.	n.d.	n.d.	n.d.	n.d.	n.d.	n.d.	n.d.	n.d.	n.d.
	A	8–23	34	12	6	8	17	18	4	1	LS	
	E	23–38	23	4	28	3	20	15	6	1	LS	
	BsC	38–58	37	15	12	6	13	12	5	0	LS	
8	Olf	0–10	n.d.	n.d.	n.d.	n.d.	n.d.	n.d.	n.d.	n.d.	n.d.	n.d.
	AE	10–33	n.d.	n.d.	n.d.	n.d.	n.d.	n.d.	n.d.	n.d.	n.d.	n.d.
	BsC1	33–40	48	13	12	12	10	3	2	0	S	
	BsC2	40–60	38	17	17	6	8	9	4	1	S	
9	Olf	0–6	n.d.	n.d.	n.d.	n.d.	n.d.	n.d.	n.d.	n.d.	n.d.	n.d.
	A	6–10	47	2	3	0	17	14	13	4	SL	
	E	10–18	24	2	4	4	18	14	27	7	SL	
	Bs	18–24	20	0	0	6	10	25	29	10	SiL	
	BC	24–60	19	2	3	1	7	13	37	18	SiL	
10	Olf	0–2	n.d.	n.d.	n.d.	n.d.	n.d.	n.d.	n.d.	n.d.	n.d.	n.d.
	A	2–6	40	24	14	4	11	5	1	1	S	
	AE	6–23	53	21	2	2	7	7	8	0	LS	
	E	23–45	37	25	10	10	1	7	6	4	LS	
	BsC	45–70	39	28	5	12	8	5	3	0	S	
11	Olf	0–3	n.d.	n.d.	n.d.	n.d.	n.d.	n.d.	n.d.	n.d.	n.d.	n.d.
	A	3–8	36	27	2	2	22	6	3	2	S	
	AE	8–16	43	1	1	4	28	11	9	3	LS	
	BsC1	16–40	32	10	1	5	15	17	18	2	SL	
	BsC2	40–65	39	28	3	0	10	10	10	0	LS	
12	Olf	0–3	n.d.	n.d.	n.d.	n.d.	n.d.	n.d.	n.d.	n.d.	n.d.	n.d.
	A	3–26	32	17	18	14	7	8	4	0	S	
	AE	26–43	14	27	5	6	10	11	19	8	SL	
	BsC	43–62	17	19	25	1	8	11	13	6	SL	
13	Ol	0–3	n.d.	n.d.	n.d.	n.d.	n.d.	n.d.	n.d.	n.d.	n.d.	n.d.
	Oh1	3–6	n.d.	n.d.	n.d.	n.d.	n.d.	n.d.	n.d.	n.d.	n.d.	n.d.
	Oh2	6–20	n.d.	n.d.	n.d.	n.d.	n.d.	n.d.	n.d.	n.d.	n.d.	n.d.
	AE	20–50	n.d.	n.d.	n.d.	n.d.	n.d.	n.d.	n.d.	n.d.	n.d.	n.d.
	BsC	50–70	38	16	2	3	15	8	14	4	LS	

Explanation: LS—loamy, SL—sandy loam, S—sand, SiL—silty loam.

## References

- Lundström, U.S.; van Breemen, N.; Bain, D. The podzolization process. A review. *Geoderma* **2000**, *94*, 91–107. [\[CrossRef\]](#)
- Mokma, D.L.; Buurman, P. *Podzols and Podzolization in Temperate Regions*; International Soil Museum: Wageningen, The Netherlands, 1982; p. 131. ISBN 9789066720114.
- Sauer, D.; Sponagel, H.; Sommer, M.; Giani, L.; Jahn, R.; Stahr, K. Podzol: Soil of the year 2007. A review on its genesis, occurrence, and functions. *J. Plant Nutr. Soil Sci.* **2007**, *170*, 581–597. [\[CrossRef\]](#)
- Vodyanitskii, Y.N.; Goryachkin, S.V.; Savichev, A.T. Distribution of rare-earth (Y, La, Ce) and other trace elements in the profiles of the podzolic soil group. *Eurasian Soil Sci.* **2011**, *44*, 500–509. [\[CrossRef\]](#)
- Miechówka, A.; Zadrożny, P.; Kowalczyk, E. Podzol soils of different climatic and vegetation belts of the Babiogórski National Park. *Polish J. Soil Sci.* **2006**, *9*, 73–79.
- Jien, S.H.; Wu, S.P.; Chen, Z.S.; Chen, T.H.; Chiu, C.Y. Characteristics and pedogenesis of podzolic forest soils along a toposequence near a subalpine lake in northern Taiwan. *Bot. Stud.* **2010**, *51*, 223–236.
- Kabała, C.; Bogacz, A.; Waroszewski, J.; Ochyra, S. Wpływ pokryw stokowych na morfologię i właściwości bielicy subalpejskiego piętra Karkonoszy. *Soil Sci. Annu.* **2008**, *59*, 90–99, (In Polish with English Summary).

8. Kabala, C.; Waroszewski, J.; Bogacz, A.; Labaz, B. On the specifics of podzols in mountain areas. *Soil Sci. Annu.* **2012**, *63*, 55–64. [[CrossRef](#)]
9. Nikodem, A.; Pavlu, L.; Kodešová, R.; Boruvka, L.; Drábek, O. Study of podzolization process under different vegetation cover in the Jizerské Hory Mts. Region. *Soil Water Res.* **2013**, *8*, 1–12. [[CrossRef](#)]
10. Musielok, Ł.; Drewnik, M.; Szymański, W.; Stolarczyk, M.; Gus-Stolarczyk, M.; Skiba, M. Conditions favoring local podzolization in soils developed from flysch regolith—A case study from the Bieszczady Mountains in southeastern Poland. *Geoderma* **2021**, *381*. [[CrossRef](#)]
11. Waroszewski, J.; Malkiewicz, M.; Mazurek, R.; Labaz, B.; Jezierski, P.; Kabala, C. Lithological discontinuities in Podzols developed from sandstone cover beds in the Stołowe Mountains (Poland). *Catena* **2015**, *126*, 11–19. [[CrossRef](#)]
12. Waroszewski, J.; Kabala, C.; Jezierski, P. Relief-induced soil differentiation at the sandstone-mudstone contact in the Stołowe Mountains, SW Poland. *Z. Geomorphol.* **2015**, *59* (Suppl. 1), 211–226. [[CrossRef](#)]
13. Waroszewski, J.; Egli, M.; Kabala, C.; Kierczak, J.; Brandova, D. Mass fluxes and clay mineral formation in soils developed on slope deposits of the Kowarski Grzbiet (Karkonosze Mountains, Czech Republic/Poland). *Geoderma* **2016**, *264*, 363–378. [[CrossRef](#)]
14. Zadrozny, P.; Halecki, W.; Gašiorek, M.; Nicia, P.; Lamorski, T. Vertical pit-mounds distribution of uprooted Norway spruce (*Picea abies* L.): Field evidence in the upper mountain belt. *iForest* **2017**, *10*, 783–787. [[CrossRef](#)]
15. Zwanzig, L.; Zwanzig, M.; Sauer, D. Outcomes of a quantitative analysis of 48 soil chronosequence studies in humid mid and high latitudes: Importance of vegetation in driving podzolization. *Catena* **2021**, *196*, 104821. [[CrossRef](#)]
16. Wilcke, W.; Baumler, R.; Deschauer, H.; Kaupenjohann, M.; Zech, W. Erratum: Small scale distribution of Al, trace elements, and PAHs in an aggregated Alpine Podzol. *Geoderma* **1996**, *71*, 19. [[CrossRef](#)]
17. Niemyska-Lukaszuk, J.; Gašiorek, M.; Miechówka, A. Kadm, nikiel, ołów i cynk w glebach i roślinach polan pasterskich Tatrzańskiego Parku Narodowego. *Zesz. Probl. Postępów Nauk Rol.* **2000**, *472*, 543–550.
18. Miechówka, A.; Niemyska-Lukaszuk, J.; Ciarkowska, K. Heavy metals in selected non-forest soils from the Tatra National Park. *Chem. Inz. Ekol.* **2002**, *9*, 1433–1438.
19. Szopka, K.; Karczewska, A.; Jezierski, P.; Kabala, C. Spatial distribution of lead in the surface layers of mountain forest soils, an example from the Karkonosze National Park, Poland. *Geoderma* **2013**, *192*, 259–268. [[CrossRef](#)]
20. Mazurek, R.; Kowalska, J.B.; Gašiorek, M.; Zadrozny, P.; Wieczorek, J. Pollution indices as comprehensive tools for evaluation of the accumulation and provenance of potentially toxic elements in soils in Ojców National Park. *J. Geochem. Explor.* **2019**, *201*, 13–30. [[CrossRef](#)]
21. Ciriaková, A. Heavy metals in the vascular plants of Tatra Mountains. *Oecologia Mont.* **2009**, *18*, 23–26.
22. Hajdúk, J. Contents of Pb, Cd, As, Fe, Cr, Zn, Cu, Ca, Mg and S in TANAP soils in relation to the effect of industrial immissions. *Zb. TANAP* **1988**, *28*, 251–261.
23. Paulo, A.; Gałaś, S.; Izakovičová, Z.; Hreško, J. Zarządzanie ochroną środowiska Tatr po obydwu stronach granicy polsko-słowackiej. In *Nauka a Zarządzanie Obszarem Tatr I Ich Otoczeniem, Tom III*; 2010; pp. 121–150, (In Polish). Available online: [https://tpn.pl/filebrowser/files/T3\\_15.pdf](https://tpn.pl/filebrowser/files/T3_15.pdf) (accessed on 5 February 2021).
24. Jaguś, A.; Skrzypiec, M. Toxic elements in mountain soils (Little Beskids, Polish Carpathians). *J. Ecol. Eng.* **2019**, *20*, 197–202. [[CrossRef](#)]
25. Korzeniowska, J.; Kraż, P. Heavy Metals Content in the Soils of the Tatra National Park Near Lake Morskie Oko and Kasprowy Wierch—A Case Study (Tatra Mts, Central Europe). *Minerals* **2020**, *10*, 1120. [[CrossRef](#)]
26. Gao, X.; Chen, C.T.A. Heavy metal pollution status in surface sediments of the coastal Bohai Bay. *Water Res.* **2012**, *46*, 1901–1911. [[CrossRef](#)] [[PubMed](#)]
27. Kowalska, J.; Mazurek, R.; Gašiorek, M.; Setlak, M.; Zaleski, T.; Waroszewski, J. Soil pollution indices conditioned by medieval metallurgical activity—A case study from Krakow (Poland). *Environ. Pollut.* **2016**, *218*, 1023–1036. [[CrossRef](#)] [[PubMed](#)]
28. Kowalska, J.B.; Mazurek, R.; Gašiorek, M.; Zaleski, T. Pollution indices as useful tools for the comprehensive evaluation of the degree of soil contamination—A review. *Environ. Geochem. Health* **2018**, *40*, 2395–2420. [[CrossRef](#)]
29. Gašiorek, M.; Kowalska, J.; Mazurek, R.; Pająk, M. Comprehensive assessment of trace element pollution in topsoil of historical urban park on an example of the Planty Park in Krakow (Poland). *Chemosphere* **2017**, *179*, 148–158. [[CrossRef](#)]
30. Mazurek, R.; Kowalska, J.; Gašiorek, M.; Zadrozny, P.; Józefowska, A.; Zaleski, T.; Kępka, W.; Tymczuk, M.; Orłowska, K. Assessment of trace elements contamination in surface layers of Roztocze National Park forest soils (SE Poland) by indices of pollution. *Chemosphere* **2017**, *168*, 839–850. [[CrossRef](#)] [[PubMed](#)]
31. Mirek, Z. Tatra Mts. and Tatra National Park—general information. In *The Nature of Tatra National Park*; Mirek, Z., Ed.; Tatrzy i Podtatrzy: Krakow, Poland, 1996; Volume 3, pp. 17–26. ISBN 83-85832-08-4.
32. Passendorfer, E. Geology. In *The Nature of Tatra National Park*; Mirek, Z., Ed.; Tatrzy i Podtatrzy: Krakow, Poland, 1996; Volume 3, pp. 9–96. ISBN 83-85832-08-4.
33. Komornicki, T.; Skiba, S. Soils. In *The Nature of Tatra National Park*; Mirek, Z., Ed.; Tatrzy i Podtatrzy: Krakow, Poland, 1996; Volume 3, pp. 215–226. ISBN 83-85832-08-4.
34. Hess, M.T. Climate. In *The Nature of Tatra National Park*; Mirek, Z., Ed.; Tatrzy i Podtatrzy: Krakow, Poland, 1996; Volume 3, pp. 53–68. ISBN 83-85832-08-4.

35. Piękoś-Mirkowa, H.; Mirek, Z. Plant communities. In *The Nature of Tatra National Park*; Mirek, Z., Ed.; Tatry i Podtatrze: Krakow, Poland, 1996; Volume 3, pp. 235–274. ISBN 83-85832-08-4.
36. Skiba, S. Studies on soils developed in different climatic and plant floors of the crystalline part of the Polish Tatra Mts. *Soil Sci. Annu.* **1977**, *28*, 205–239. (In Polish)
37. PAN, Polish Geological Society. *Geological Map of Polish Tatra Mts. 1:30,000*; Geological Publishing: Warszawa, Poland, 1979.
38. FAO. *Guidelines for Soil Description*, 4th ed.; Food and Agriculture Organization of the United Nations: Rome, Italy, 2006; p. 109. ISBN 92-5-105521-1.
39. Munsell. *Standard Soil Color Charts*; 1975.
40. IUSS Working Group WRB. *World Reference Base for Soil Resources 2015. International Soil Classification System for Naming Soils and Creating Legends for Soil Maps*; WRB: Greenwich, CT, USA, 2014; ISBN 9789251083697.
41. van Reeuwijk, L.P. *Procedures for Soil Analysis, 6th ed*; ISRIC: Wageningen, The Netherlands, 2002.
42. Polish Standard. *PN-ISO 14235:2003 Soil Quality-Determination of Organic Carbon by Oxidation with Dichromate (VI) in a Sulfuric Acid (VI) Medium*; Polish Committee for Standardization: Warszawa, Poland, 2003. (In Polish)
43. Polish Standard. *Polish Standard, PN-ISO 11261:2002 Soil Quality-Determination of Total Nitrogen-Modified Kjeldahl Method*; Polish Committee for Standardization: Warszawa, Poland, 2002. (In Polish)
44. Ostrowska, A.; Gawlinski, S.; Szczubiałka, Z. *Methods of Analysis and Assessment of Soil and Plant Properties. A Catalogue*; Institute of Environmental Protection e National Research Institute: Warsaw, Poland, 1991. (In Polish)
45. Håkanson, L. An ecological risk index for aquatic pollution control: A sedimentological approach. *Water Res.* **1980**, *14*, 975–1001. [[CrossRef](#)]
46. Müller, G. Index of geoaccumulation in sediments of the Rhine River. *Geojournal* **1969**, *2*, 108–118.
47. Gałuszka, A.; Migaszewski, Z. Geochemical background: An environmental perspective. *Mineralogia* **2011**, *42*, 7–17. [[CrossRef](#)]
48. Jansen, B.; Nierop, K.G.J.; Verstraten, J.M. Mechanisms controlling the mobility of dissolved organic matter, aluminium and iron in podzol B horizons. *Eur. J. Soil Sci.* **2005**, *56*, 537–550. [[CrossRef](#)]
49. Drewnik, M. *Geomorfologiczne Uwarunkowania Rozwoju Pokrywy Glebowej W Obszarach Górskich Na Przykładzie Tatr*; Wydawnictwo Uniwersytetu Jagiellońskiego: Kraków, Poland, 2008; p. 120. ISBN 978-83-233-2451-5.
50. Miechówka, A.; Zaleski, T.; Kowalczyk, E. Distribution of iron and aluminum forms as an indicator of present-day soil-forming processes in soil profiles under wooded spruce *Plagiothecio-Piccetum tatricum* in the Gorce Mts. (southern Poland). *Soil Sci. Annu.* **2015**, *66*, 125–132. [[CrossRef](#)]
51. Oleksynowa, K.; Skiba, S.; Miechówka, A. Soils formed on granitoids in *Pinetum mughii* communities in the Tatra Mts. Part I. Morphological and chemical properties. *Soil Sci. Annu.* **1983**, *34*, 227–249.
52. Konecka-Betley, K. Reconstruction of late Pleistocene and Holocene pedological processes in the central Poland. *Soil Sci. Annu.* **2001**, *52*, 99–118, (In Polish with English Summary).
53. Miles, J. The pedogenic effects of different species and vegetation types and the implications of succession. *J. Soil Sci.* **1985**, *36*, 571–584. [[CrossRef](#)]
54. Waroszewski, J.; Kalinski, K.; Malkiewicz, M.; Mazurek, R.; Kozłowski, G.; Kabala, C. Pleistocene–Holocene cover-beds on granite regolith as parent material for Podzols—An example from the Sudeten Mountains. *Catena* **2013**, *104*, 161–173. [[CrossRef](#)]
55. Raczuk, J. Heavy metals in the forest soils of the South Podlasie Lowland. *Acta Agroph.* **2001**, *51*, 263–274.
56. Jonczak, J. Vertical distribution of Cu, Ni and Zn in Brunic Arenosols and Gleyic Podzols of the supra-flood terrace of the Słupia River as affected by litho-pedogenic factors. *For. Res. Pap.* **2015**, *75*, 333–341. [[CrossRef](#)]
57. MacDonald, J.D.; Hendershot, W.H. Spatial variability of trace metals in Podzols of northern forest ecosystems: Sampling implications. *Can. J. Soil Sci.* **2003**, *83*, 581–587. [[CrossRef](#)]
58. Starr, M.; Lindroosa, A.J.; Ukonmaanaho, L.; Tarvainen, T.; Tanskanen, H. Weathering release of heavy metals from soil in comparison to deposition, litter fall and leaching fluxes in a remote, boreal coniferous forest. *Appl. Geochem.* **2003**, *18*, 607–613. [[CrossRef](#)]
59. Waroszewski, J.; Sprafke, T.; Kabala, C.; Musztyfaga, E.; Łabaz, B.; Woźniczka, P. Aeolian silt contribution to soils on mountain slopes (Mt. Ślęza, southwest Poland). *Quat. Res.* **2018**, *89*, 702–717. [[CrossRef](#)]
60. Souchez, R.A. The Origin of Morainic Deposits and the Characteristics of Glacial Erosion in the Western Sør-Rondane, Antarctica. *J. Glaciol.* **1966**, *6*, 249–254. [[CrossRef](#)]
61. Zhu, H.; Zhao, Y.; Nan, F.; Duan, Y.; Bi, R. Relative influence of soil chemistry and topography on soil available micronutrients by structural equation modeling. *J. Soil Sci. Plant Nutr.* **2016**, *16*, 1038–1051. [[CrossRef](#)]
62. Henkner, J.; Ahlrichs, J.; Downey, S.; Fuchs, M.; James, B.; Junge, A.; Knopf, T.; Scholten, T.; Kühn, P. Archaeopedological analysis of colluvial deposits in favourable and unfavourable areas: Reconstruction of land use dynamics in SW Germany. *R. Soc. Open Sci.* **2018**, *5*. [[CrossRef](#)]
63. De Santo, A.V.; Fierro, A.; Berg, B.; Rutigliano, F.A.; De Marco, A. Heavy metals and litter decomposition in coniferous forests. *Dev. Soil Sci.* **2002**, *28*, 63–78. [[CrossRef](#)]
64. Naumov, V.D.; Kamennyh, N.L.; Lebedev, A.V.; Gemonov, A.V.; Gemonova, P.S. Heavy metals in sod-podzolic soils under forest stands of Moscow. *IOP Conf. Ser. Earth Environ. Sci.* **2020**, *421*. [[CrossRef](#)]
65. McEnroe, N.A.; Helmissaari, H.S. Decomposition of coniferous forest litter along a heavy metal pollution gradient, south-west Finland. *Environ. Pollut.* **2001**, *113*, 11–18. [[CrossRef](#)]

66. Falkengren-Grerup, U. Soil acidification and vegetation changes in deciduous forest in southern Sweden. *Oecologia* **1986**, *70*, 339–347. [[CrossRef](#)] [[PubMed](#)]
67. Barkan, V.S.; Lyanguzova, I.V. Changes in the Degree of Contamination of Organic Horizons of Al–Fe–Humus Podzols upon a Decrease in Aerotechnogenic Loads, the Kola Peninsula. *Eurasian Soil Sci.* **2018**, *51*, 327–335. [[CrossRef](#)]
68. Steinnes, E. Impact of Long-range Atmospheric Transport of Heavy Metals to the Terrestrial Environment in Norway. *Lead Mercur. Cadmium Arsen. Environ.* **1987**, 107–117.
69. Nowack, B.; Obrecht, J.M.; Schluep, M.; Schulin, R.; Hansmann, W.; Köppel, V. Elevated lead and zinc contents in remote alpine soils of the Swiss National Park. *J. Environ. Qual.* **2001**, *30*, 919–926. [[CrossRef](#)]
70. Skłodowski, P.; Maciejewska, A.; Szafranek, A. Podzolization process effect on distribution of traces elements in profile of podzol soils. *Soil Sci. Annu.* **1988**, *39*, 113–128, (In Polish with English Summary).
71. Stobiński, M.; Kubica, B. Chemometric analysis of <sup>137</sup>Cs activity and heavy metals distribution in the Tatras' soil. *Int. J. Environ. Sci. Technol.* **2017**, *14*, 1217–1224. [[CrossRef](#)]
72. Grodzińska, K.; Szarek, G.; Godzik, B. Heavy metal deposition in Polish national parks—Changes during ten years. *Water Air Soil Pollut.* **1990**, *49*, 409–419. [[CrossRef](#)]
73. Karczewska, A.; Szopka, K.; Kabała, C.; Bogacz, A. Zinc and lead in forest soils of Karkonosze National Park. *Polish J. Environ. Stud.* **2006**, *15*, 336–342.
74. Ghazaryan, K.A.; Movsesyan, H.S.; Ghazaryan, N.P. Heavy Metals in the Soils of the Mining Regions of Kajaran, Armenia: A Preliminary Definition of Contaminated Areas. *Acad. J. Sci.* **2017**, *7*, 421–429.
75. Pacyna, J.M.; Pacyna, E.G. An assessment of global and regional emissions of trace metals to the atmosphere from anthropogenic sources worldwide. *Environ. Rev.* **2001**, *44*, 269–298. [[CrossRef](#)]
76. Steinnes, E.; Allen, R.O.; Petersen, H.M.; Rambaek, J.P.; Varskog, P. Evidence of large scale heavy-metal contamination of natural surface soils in Norway from long-range atmospheric transport. *Sci. Total Environ.* **1997**, *205*, 255–266. [[CrossRef](#)]